

Dispersion relations for $B^- \rightarrow \ell^- \bar{\nu}_\ell \ell'^- \ell'^+$ form factors

Stephan Kürten,^{1,*} Marvin Zanke^{2,†} Bastian Kubis^{2,‡} and Danny van Dyk^{1,3,§}

¹*Physik Department (T31), Technische Universität München, 85748 Garching, Germany*

²*Helmholtz-Institut für Strahlen- und Kernphysik (Theorie) and Bethe Center for Theoretical Physics, Universität Bonn, 53115 Bonn, Germany*

³*Institute for Particle Physics Phenomenology and Department of Physics, Durham University, Durham DH1 3LE, United Kingdom*



(Received 26 October 2022; accepted 6 February 2023; published 17 March 2023)

Using dispersive methods, we study the $B \rightarrow \gamma^*$ form factors underlying the decay $B^- \rightarrow \ell^- \bar{\nu}_\ell \ell'^- \ell'^+$. We discuss the ambiguity that arises from a separation of the full $B^- \rightarrow \ell^- \bar{\nu}_\ell \ell'^- \ell'^+$ amplitude into a hadronic tensor and a final-state-radiation piece, including effects from nonvanishing lepton masses. For the eligibility of a dispersive treatment, we propose a decomposition of the hadronic part that leads to four form factors that are free of kinematic singularities. By establishing a set of dispersion relations, we then relate the $B \rightarrow \gamma^*$ form factors to the well-known $B \rightarrow V$, $V = \omega(782), \rho(770)$, analogs. Using the combination of a series expansion in a conformal variable and a vector-meson-dominance ansatz to parametrize the $B \rightarrow \gamma^*$ form factors, we infer the values of the associated unknown parameters from the available input on $B \rightarrow V$. The phenomenological application of our formalism includes the determination of the branching ratios and forward-backward asymmetries of the process $B^- \rightarrow \ell^- \bar{\nu}_\ell \ell'^- \ell'^+$.

DOI: [10.1103/PhysRevD.107.053006](https://doi.org/10.1103/PhysRevD.107.053006)

I. INTRODUCTION

The radiative leptonic decay $B^- \rightarrow \ell^- \bar{\nu}_\ell \gamma$ is widely considered to be the best source of information on the leading-twist B -meson light-cone distribution amplitude (LCDA) by elucidating the inner structure of the B meson [1–3]. However, measurements of this decay are likely only possible at the ongoing Belle II experiment and not at the LHC experiments, primarily the LHCb. This precludes leveraging the upcoming large datasets at the LHC, which will become available from run 3 onwards. The four-lepton decay of the B meson, $B^- \rightarrow \ell^- \bar{\nu}_\ell \ell'^- \ell'^+$, with $\ell' \neq \ell$, $\ell^{(\prime)} = e, \mu$, has been identified as a suitable candidate for studies at both Belle II and the LHC experiments. This decay has been studied to some extent in the literature, with a variety of models for the relevant $B \rightarrow \gamma^*$ form factors [4–7]. However, its usefulness to extract B -meson LCDA parameters is hampered by the need for a

description of a virtual photon in the timelike region, which requires careful treatment.

We propose a dispersive approach for $B \rightarrow \gamma^*$, which is based on the fundamental principles of analyticity and unitarity. Dispersive analyses in the timelike region are commonly done for low-energy processes, such as the pion vector form factor; see, for instance, Ref. [8] and references therein. Here, we apply methods originally developed for these processes to hadronic transition form factors of B mesons. For future analyses, our approach has the potential to enable the transfer of information from the region of timelike photon momentum to the spacelike region, where the sensitivity to the LCDA parameters is less affected by soft interactions [3]. We relate the isoscalar and isovector components of the $B \rightarrow \gamma^*$ transition inherent to the hadronic part of the amplitude through $B^- \rightarrow \ell^- \bar{\nu}_\ell \gamma^* (\rightarrow \ell'^- \ell'^+)$ to available input on $B \rightarrow \omega \equiv \omega(782)$ and $B \rightarrow \rho \equiv \rho(770)$ [9] via a set of dispersion relations in the photon momentum. Although we use a vector-meson-dominance (VMD) ansatz in this work, our results provide the groundwork for more sophisticated future analyses. Using dispersion relations requires the form factors to be free of kinematic singularities. We modify the well-known Bardeen-Tung-Tarrach (BTT) [10,11] procedure, which has not been designed for hadronic form factors in weak transitions, to obtain such a set of form factors. At this, we face a problem: the separation of the amplitude into a hadronic term—containing the nonperturbative dynamics of the process—and a final-state-radiation (FSR) term turns out

*stephan.kuerten91@gmail.com

†zanke@hiskp.uni-bonn.de

‡kubis@hiskp.uni-bonn.de

§danny.van.dyk@gmail.com

Published by the American Physical Society under the terms of the [Creative Commons Attribution 4.0 International license](https://creativecommons.org/licenses/by/4.0/). Further distribution of this work must maintain attribution to the author(s) and the published article's title, journal citation, and DOI. Funded by SCOAP³.

to be ambiguous; the two terms are not individually gauge invariant but only their sum is. A further issue is the lack of definite angular-momentum and parity quantum numbers of the form factors. Our modification to the BTT procedure addresses this issue, and we take special care not to spoil the singularity-free structure.

To ensure a consistent treatment of lepton-mass effects, we work with nonzero lepton masses throughout our analysis; taking the limit $m_{\ell^{(\nu)}} \rightarrow 0$ remains possible. While the considerations in this article are mostly restricted to the decay of a negatively charged B meson, the decay of a positively charged B meson can be calculated in complete analogy, with some minor adjustments to the formulas given here and completely equivalent numerical results.

The outline of this article is as follows: in Sec. II, we introduce the Lagrangian of the weak effective theory (WET) that describes semileptonic $b \rightarrow u\ell\bar{\nu}$ transitions. The amplitude for $B^- \rightarrow \ell^-\bar{\nu}_\ell\gamma^*(\rightarrow \ell'^-\ell'^+)$ and its decomposition into a hadronic tensor and an FSR piece is discussed in Sec. III. Using our modified BTT procedure, the hadronic tensor is then parametrized in terms of four form factors that are free of kinematic singularities in Sec. IV, where the ambiguity arising from the separation of the full amplitude is a subject of special attention. In Sec. V, we establish a set of dispersion relations that relate the $B^- \rightarrow \gamma^*$ transition inherent to the hadronic part of the amplitude to available input on $B^- \rightarrow V$ form factors, $V = \omega, \rho$, and provide predictions for the $B^- \rightarrow \gamma^*$ form factors. Using these predictions, we present numerical results for the branching ratios and forward-backward (FB) asymmetries of the process $B^- \rightarrow \ell^-\bar{\nu}_\ell\ell'^-\ell'^+$ in Sec. VI. We conclude and give a brief outlook in Sec. VII. Some supplementary material is outsourced to Appendixes A–G.

II. WEAK EFFECTIVE THEORY

At the energy scale of the B meson, the standard model's (SM's) flavor-changing processes are conveniently described within an effective field theory [12,13]. The leading terms in this theory arise at mass dimension six, with higher-dimensional operators being suppressed by at least $m_B^2/M_W^2 \approx 0.4\%$. Moreover, such an effective field theory allows us to transparently include potential effects beyond the SM as long as new matter fields and mediators live above the scale of electroweak symmetry breaking. For $b \rightarrow u\ell\bar{\nu}_\ell$ transitions in particular, we use the effective Lagrangian

$$\mathcal{L}_{\text{WET}}^{ub\ell\nu} = \frac{4G_F}{\sqrt{2}} V_{ub} \sum_i \mathcal{C}_i^{ub\ell\nu} \mathcal{O}_i^{ub\ell\nu} + \text{H.c.}, \quad (1)$$

where G_F is the Fermi constant as measured in muon decays, V_{ub} is the Cabibbo-Kobayashi-Maskawa (CKM) matrix element for the $b \rightarrow u$ transition, and $\mathcal{C}_i^{ub\ell\nu} \equiv \mathcal{C}_i^{ub\ell\nu}(\mu)$ are the so-called Wilson coefficients at the scale μ that multiply the local field operators $\mathcal{O}_i^{ub\ell\nu} \equiv \mathcal{O}_i^{ub\ell\nu}(x)$. A convenient basis of operators up to dimension six and with only left-handed neutrinos is given by

$$\begin{aligned} \mathcal{O}_{V,L(R)}^{ub\ell\nu} &= [\bar{u}(x)\gamma^\mu P_{L(R)}b(x)][\bar{\ell}(x)\gamma_\mu P_L\nu_\ell(x)], \\ \mathcal{O}_{S,L(R)}^{ub\ell\nu} &= [\bar{u}(x)P_{L(R)}b(x)][\bar{\ell}(x)P_L\nu_\ell(x)], \\ \mathcal{O}_T^{ub\ell\nu} &= [\bar{u}(x)\sigma^{\mu\nu}b(x)][\bar{\ell}(x)\sigma_{\mu\nu}P_L\nu_\ell(x)], \end{aligned} \quad (2)$$

where, in the SM, $\mathcal{C}_{V,L}^{ub\ell\nu}|_{\text{SM}} = 1 + \mathcal{O}(\alpha_e)$ and $\mathcal{C}_i^{ub\ell\nu}|_{\text{SM}} = 0$ for all other corresponding Wilson coefficients. Here, $P_{L/R} = (1 \mp \gamma_5)/2$ are the projection operators onto the left- and right-chiral components and $\alpha_e = e^2/(4\pi)$ is the fine-structure constant. To leading order in the electromagnetic (EM) interaction, matrix elements of the above operators factorize into matrix elements of a purely hadronic and a purely leptonic current. In this work, we limit ourselves to the SM operator $\mathcal{O}_{V,L}^{ub\ell\nu}$ and—to a lesser extent—the scalar operator $\mathcal{O}_{S,L}^{ub\ell\nu}$.

III. HADRONIC TENSOR

We study the decay $B^-(p) \rightarrow \ell^-(p_\ell)\bar{\nu}_\ell(p_\nu)\gamma^*(q)$, $k = p_\ell + p_\nu$, whose amplitude in the SM reads [1]

$$\mathcal{M}(B^- \rightarrow \ell^-\bar{\nu}_\ell\gamma^*) = \frac{4G_F V_{ub}}{\sqrt{2}} \langle \ell^-\bar{\nu}_\ell\gamma^* | \mathcal{O}_{V,L}^{ub\ell\nu} | B^- \rangle \quad (3)$$

up to corrections of $\mathcal{O}(\alpha_e)$. It is convenient to write the WET operator in terms of the leptonic and hadronic weak currents $J_W^\nu(x) = \bar{\ell}(x)\gamma^\nu(1 - \gamma_5)\nu_\ell(x)$ and $J_H^\nu(x) = \bar{u}(x)\gamma^\nu(1 - \gamma_5)b(x)$ according to

$$\mathcal{O}_{V,L}^{ub\ell\nu} = \frac{1}{4} J_{H_L}^\nu(0) J_W^\nu(0). \quad (4)$$

At the level of the WET, there are two possible diagrammatic ways for the emission of the (virtual) photon: either from the constituents of the B meson or from the charged final-state lepton; the respective diagrams are shown in Fig. 1.

At leading order in the EM coupling, the hadronic matrix element on the right-hand side of Eq. (3) can be written as

$$\begin{aligned}
\langle \ell^- \bar{\nu}_\ell \gamma^* | J_{\text{H}\nu}(0) J_{\text{W}}^\nu(0) | B^- \rangle &= e \epsilon_\mu^* \left[\langle \ell^- \bar{\nu}_\ell | J_{\text{W}\nu}(0) | 0 \rangle \int d^4x e^{iqx} \langle 0 | T \{ J_{\text{EM}}^\mu(x) J_{\text{H}}^\nu(0) \} | B^- \rangle \right. \\
&\quad \left. + \langle 0 | J_{\text{H}\nu}(0) | B^- \rangle \int d^4x e^{iqx} \langle \ell^- \bar{\nu}_\ell | T \{ J_{\text{EM}}^\mu(x) J_{\text{W}}^\nu(0) \} | 0 \rangle \right] \\
&= e \epsilon_\mu^* \left[Q_B L_\nu T_{\text{H}}^{\mu\nu}(k, q) - i f_B p_\nu \int d^4x e^{iqx} \langle \ell^- \bar{\nu}_\ell | T \{ J_{\text{EM}}^\mu(x) J_{\text{W}}^\nu(0) \} | 0 \rangle \right] \\
&= e \epsilon_\mu^* [Q_B L_\nu T_{\text{H}}^{\mu\nu}(k, q) + Q_\ell T_{\text{FSR}}^\mu(p_\ell, p_\nu, q)], \tag{5}
\end{aligned}$$

where e is the elementary charge and $\epsilon_\mu^* \equiv \epsilon_\mu^*(q; \lambda)$ the polarization vector of the outgoing photon with momentum q and polarization λ . Furthermore, f_B is the decay constant of the B -meson, $\langle 0 | \bar{u}(0) \gamma^\nu \gamma_5 b(0) | B^- \rangle = i f_B p^\nu$, and

$$J_{\text{EM}}^\mu(x) = \bar{q}(x) Q \gamma^\mu q(x) + \sum_\ell Q_\ell \bar{\ell}(x) \gamma^\mu \ell(x) \tag{6}$$

the EM current, with $q(x) = (u(x), d(x), s(x), c(x), b(x))^T$, $Q = \text{diag}[2/3, -1/3, -1/3, 2/3, -1/3]$ the quark charge matrix, and $Q_B = -1 = Q_\ell$ the charge of the B meson and lepton in units of e . With the aim to render the transfer of our analysis to the positively charged channel more transparent, we will explicitly retain factors of $Q_B = Q_\ell$ in our formulas; it is, however, to be kept in mind that further modifications of the spinor structure apply beyond this simple alteration. In Eq. (5), we moreover abbreviate the leptonic matrix element $L_\nu = \bar{u}_\ell \gamma_\nu (1 - \gamma_5) v_{\bar{\nu}}$ and introduce the hadronic tensor $T_{\text{H}}^{\mu\nu}(k, q)$,

$$Q_B T_{\text{H}}^{\mu\nu}(k, q) = \int d^4x e^{iqx} \langle 0 | T \{ J_{\text{EM}}^\mu(x) J_{\text{H}}^\nu(0) \} | B^- \rangle, \tag{7}$$

and the FSR tensor $T_{\text{FSR}}^\mu(p_\ell, p_\nu, q)$,

$$\begin{aligned}
Q_\ell T_{\text{FSR}}^\mu(p_\ell, p_\nu, q) \\
= -i f_B p_\nu \int d^4x e^{iqx} \langle \ell^- \bar{\nu}_\ell | T \{ J_{\text{EM}}^\mu(x) J_{\text{W}}^\nu(0) \} | 0 \rangle. \tag{8}
\end{aligned}$$

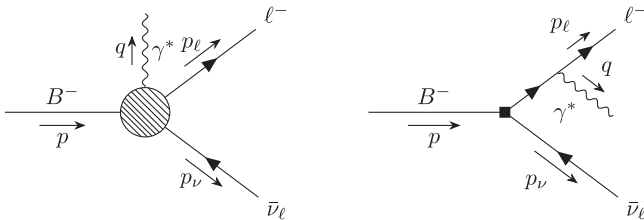


FIG. 1. The diagrams contributing to the decay $B^- \rightarrow \ell^- \bar{\nu}_\ell \ell'^*$ at dimension six in the WET on the hadronic level: (left) pole and cut contributions of $T_{\text{H}}^{\mu\nu}(k, q)$, e.g., from the intermediate states B in k^2 or $\pi\pi$ in q^2 , and (right) emission from the charged final-state lepton in $T_{\text{FSR}}^\mu(p_\ell, p_\nu, q)$. The hadronic tensor $T_{\text{H}}^{\mu\nu}(k, q)$ and FSR tensor $T_{\text{FSR}}^\mu(p_\ell, p_\nu, q)$ are defined in Eqs. (7) and (8), respectively. Note that an effective four-particle vertex is discarded here, since it contributes at dimension eight in the WET.

While the hadronic tensor $T_{\text{H}}^{\mu\nu}(k, q)$ describes the genuinely nonperturbative physics of the process, $T_{\text{FSR}}^\mu(p_\ell, p_\nu, q)$ comprises the FSR from the charged lepton and can be reduced to the B -meson decay constant f_B and an entirely perturbative remainder. The former can be decomposed into a set of Lorentz structures and associated scalar-valued functions, which are commonly referred to as the $B \rightarrow \gamma^*$ form factors. The purpose of this work is to study these form factors within a dispersive framework, which requires knowledge of their singularity structure in the two independent kinematic variables and of the form factors' asymptotic behavior (see Sec. IV).

For the FSR tensor in the case of a massless charged lepton, one finds the remarkably simple result [1,4,5,14,15]

$$T_{\text{FSR},0}^\mu(p_\ell, p_\nu, q) = f_B L^\mu. \tag{9}$$

The case of nonzero mass leads to the more intricate formula [16,17]

$$\begin{aligned}
T_{\text{FSR},m_\ell}^\mu(p_\ell, p_\nu, q) \\
= f_B \left[L^\mu + m_\ell \bar{u}_\ell \frac{2p_\ell^\mu + \gamma^\mu \not{q}}{(p_\ell + q)^2 - m_\ell^2} (1 - \gamma_5) v_{\bar{\nu}} \right]. \tag{10}
\end{aligned}$$

For our purpose, it proves convenient to bring the FSR contribution into such a form that it shares a common factor of L_ν with its hadronic counterpart, i.e.,

$$\begin{aligned}
\langle \ell^- \bar{\nu}_\ell \gamma^* | J_{\text{W}}^\nu(0) J_{\text{H}\nu}(0) | B^- \rangle \\
= e Q_B \epsilon_\mu^* [T_{\text{H}}^{\mu\nu}(k, q) + T_{\text{FSR}}^{\mu\nu}(p_\ell, p_\nu, q)] L_\nu. \tag{11}
\end{aligned}$$

It is straightforward to achieve such a description for the massless case, $m_\ell = 0$, Eq. (9). For the massive case, $m_\ell \neq 0$, we make use of the Chisholm identity [18]

$$i \epsilon^{\mu\nu\rho\sigma} \gamma_\sigma \gamma_5 = \gamma^\mu \gamma^\nu \gamma^\rho - g^{\mu\nu} \gamma^\rho + g^{\mu\rho} \gamma^\nu - g^{\nu\rho} \gamma^\mu, \tag{12}$$

with the convention $\epsilon^{0123} = +1$. From this, we obtain

$$T_{\text{FSR}}^{\mu\nu}(p_\ell, p_\nu, q) = f_B \left[g^{\mu\nu} + \frac{2p_\ell^\mu p_\ell^\nu + p_\ell^\mu q^\nu + q^\mu p_\ell^\nu - (p_\ell \cdot q)g^{\mu\nu} + i\epsilon^{\mu\nu\rho\sigma}(p_\ell)_\rho q_\sigma}{(p_\ell + q)^2 - m_\ell^2} \right], \quad (13)$$

which is valid only when contracted with the leptonic matrix element L_ν .¹

Because of gauge invariance, the full amplitude complies with the Ward identity

$$q_\mu [T_{\text{H}}^{\mu\nu}(k, q) + T_{\text{FSR}}^{\mu\nu}(p_\ell, p_\nu, q)] L_\nu = 0. \quad (14)$$

However, the hadronic and FSR tensor are not individually gauge invariant but satisfy [1,4,5]

$$\begin{aligned} q_\mu T_{\text{H}}^{\mu\nu}(k, q) &= -f_B(k+q)^\nu, \\ q_\mu T_{\text{FSR}}^{\mu\nu}(p_\ell, p_\nu, q) &= f_B(k+q)^\nu, \end{aligned} \quad (15)$$

so that gauge invariance only holds for the sum of both contributions. Based on Eq. (15), we split the hadronic tensor into a homogeneous part and an inhomogeneous part by means of $T_{\text{H}}^{\mu\nu}(k, q) = T_{\text{H,hom}}^{\mu\nu}(k, q) + T_{\text{H,inhom}}^{\mu\nu}(k, q)$, which obey

$$\begin{aligned} q_\mu T_{\text{H,hom}}^{\mu\nu}(k, q) &= 0, \\ q_\mu T_{\text{H,inhom}}^{\mu\nu}(k, q) &= -f_B(k+q)^\nu. \end{aligned} \quad (16)$$

We have not yet made any choice of Lorentz decomposition for $T_{\text{H}}^{\mu\nu}(k, q)$ or its (in)homogeneous part. In Appendix A, we demonstrate that any choice for the decomposition of the hadronic tensor leads to the relation

$$k_\nu T_{\text{H,hom}}^{\mu\nu}(k, q) = T_P^\mu(k, q) + f_B(k+q)^\mu - k_\nu T_{\text{H,inhom}}^{\mu\nu}(k, q), \quad (17)$$

where the pseudoscalar tensor $T_P^\mu(k, q)$ is defined in terms of the pseudoscalar weak current $J_P(x) = \bar{u}(x)\gamma_5 b(x)$ via

$$\begin{aligned} Q_B T_P^\mu(k, q) &= (m_b + m_u) \int d^4x e^{iqx} \langle 0 | T \{ J_{\text{EM}}^\mu(x) J_P(0) \} | B^- \rangle, \end{aligned} \quad (18)$$

with m_b and m_u the $\overline{\text{MS}}$ masses of the b - and u -quarks. As also shown in Appendix A, this tensor is not gauge invariant but, similar to Eq. (15), fulfills

$$q_\mu T_P^\mu(k, q) = -f_B m_B^2. \quad (19)$$

¹Note that one can, in principle, further make the replacement $p_\ell^\nu \rightarrow k^\nu$ in Eq. (13) by virtue of the Dirac equation for the neutrino.

For this reason, we proceed in analogy to Eq. (16) and split $T_P^\mu(k, q) = T_{P,\text{hom}}^\mu(k, q) + T_{P,\text{inhom}}^\mu(k, q)$, where

$$\begin{aligned} q_\mu T_{P,\text{hom}}^\mu(k, q) &= 0, \\ q_\mu T_{P,\text{inhom}}^\mu(k, q) &= -f_B m_B^2. \end{aligned} \quad (20)$$

In this work, we additionally impose that the homogeneous part of the hadronic tensor fulfills

$$k_\nu T_{\text{H,hom}}^{\mu\nu}(k, q) \stackrel{!}{=} T_{P,\text{hom}}^\mu(k, q), \quad (21)$$

which, using Eq. (17), leads to the condition

$$T_{P,\text{inhom}}^\mu(k, q) + f_B(k+q)^\mu - k_\nu T_{\text{H,inhom}}^{\mu\nu}(k, q) = 0. \quad (22)$$

This choice is natural because it relates one of the hadronic form factors of the axial-vector current with that of the pseudoscalar current, as is the case for hadronic form factors in other weak transitions, too.

The tensors $T_{\text{H}}^{\mu\nu}(k, q)$ and $T_{\text{FSR}}^{\mu\nu}(p_\ell, p_\nu, q)$ emerge in predictions for the decay $B^-(p) \rightarrow \ell^-(p_\ell) \bar{\nu}_\ell(p_\nu) \ell'^-(q_1) \ell'^+(q_2)$, with $\ell' \neq \ell$, $q = q_1 + q_2$,

$$\begin{aligned} \mathcal{M}(B^- \rightarrow \ell^- \bar{\nu}_\ell \ell'^- \ell'^+) &= \frac{4G_F V_{ub}}{\sqrt{2}} \langle \ell^- \bar{\nu}_\ell \ell'^- \ell'^+ | \mathcal{O}_{V,L}^{ub\ell\nu} | B^- \rangle \\ &= \frac{G_F V_{ub} e^2}{\sqrt{2} q^2} Q_B [T_{\text{H}}^{\mu\nu}(k, q) + T_{\text{FSR}}^{\mu\nu}(p_\ell, p_\nu, q)] l_\mu L_\nu, \end{aligned} \quad (23)$$

where we abbreviate the leptonic matrix element $l_\mu = \bar{u}_{\ell'} \gamma_\mu v_{\bar{\ell}'}$. The discussion of the decay with identical lepton flavors, $\ell' = \ell$, is more involved [4,19], since an additional diagram has to be taken into account due to the interchangeability of two final-state fermions, which is beyond the scope of this article.

IV. $B \rightarrow \gamma^*$ FORM FACTORS

We develop a method that closely resembles the BTT procedure [10,11] to parametrize the homogeneous part of the hadronic tensor (see Appendix B). Compared to the BTT procedure, our method has the advantage that the emerging form factors have definite angular-momentum and parity quantum numbers. Our result reads

TABLE I. The ansätze for the inhomogeneous part of the hadronic tensor used in the literature expressed as in Eq. (25) for specific choices of the coefficients a , b , and c . Also shown are the resulting inhomogeneous parts of the pseudoscalar tensor, Eq. (26), and its associated coefficient d , Eq. (27). The basis for the homogeneous part of the hadronic tensor differs from our choice, Eq. (24), in some of the references. A thorough discussion of the various choices can be found in the main text.

Label	a	b	c	$T_{\text{H,inhom}}^{\mu\nu}(k, q)$	d	$T_{P,\text{inhom}}^\mu(k, q)$	References
\mathcal{A}	1	$\frac{2(k \cdot q)}{2(k \cdot q) + q^2}$	0	$-f_B [g^{\mu\nu} + \frac{(2k^\mu + q^\mu)k^\nu}{2(k \cdot q) + q^2}]$	$\frac{2(k \cdot q)}{2(k \cdot q) + q^2}$	$-f_B m_B^2 \frac{2k^\mu + q^\mu}{2(k \cdot q) + q^2}$	[15–17,20]
\mathcal{B}	0	$\frac{k \cdot q}{k \cdot q + q^2}$	$\frac{k \cdot q}{k \cdot q + q^2}$	$-f_B \frac{(k+q)^\mu (k+q)^\nu}{k \cdot q + q^2}$	$\frac{k \cdot q}{k \cdot q + q^2}$	$-f_B m_B^2 \frac{k^\mu + q^\mu}{k \cdot q + q^2}$	[1,14]
\mathcal{C}	0	1	1	$-f_B \frac{k^\mu (k+q)^\nu}{k \cdot q}$	$\frac{2(k \cdot q) + k^2}{2(k \cdot q) + k^2 + q^2}$	$-f_B [m_B^2 \frac{k^\mu}{k \cdot q} - \frac{q^2 k^\mu - (k \cdot q) q^\mu}{k \cdot q}]$	[4]
\mathcal{D}	0	0	0	$-f_B \frac{q^\mu (k+q)^\nu}{q^2}$	$\frac{k \cdot q}{2(k \cdot q) + k^2 + q^2}$	$-f_B [m_B^2 \frac{q^\mu}{q^2} - \frac{(k \cdot q) q^\mu - q^2 k^\mu}{q^2}]$	[5]

$$T_{\text{H,hom}}^{\mu\nu}(k, q) = \frac{1}{m_B} [(k \cdot q) g^{\mu\nu} - k^\mu q^\nu] \mathcal{F}_1(k^2, q^2) + \frac{1}{m_B} \left[\frac{q^2}{k^2} k^\mu k^\nu - \frac{k \cdot q}{k^2} q^\mu k^\nu + q^\mu q^\nu - q^2 g^{\mu\nu} \right] \mathcal{F}_2(k^2, q^2) + \frac{1}{m_B} \left[\frac{k \cdot q}{k^2} q^\mu k^\nu - \frac{q^2}{k^2} k^\mu k^\nu \right] \mathcal{F}_3(k^2, q^2) + \frac{i}{m_B} \epsilon^{\mu\nu\rho\sigma} k_\rho q_\sigma \mathcal{F}_4(k^2, q^2), \quad (24)$$

where the form factors $\mathcal{F}_1(k^2, q^2)$ and $\mathcal{F}_2(k^2, q^2)$ have axial-vector, $\mathcal{F}_3(k^2, q^2)$ has pseudoscalar, and $\mathcal{F}_4(k^2, q^2)$ vector quantum numbers with respect to the weak current.² Assuming no modification due to the inhomogeneous part $T_{\text{H,inhom}}^{\mu\nu}(k, q)$, our form factors are free of kinematic singularities in k^2 and q^2 as well as kinematic zeros in q^2 . However, to ensure a finite amplitude at $k^2 = 0$, the relation $\mathcal{F}_2(0, q^2) = \mathcal{F}_3(0, q^2)$ must hold for all q^2 . The factors of m_B and the imaginary unit in Eq. (24) render the form factors dimensionless and—with the phase of the B meson chosen appropriately—real-valued below the onset of the first branch cut.

The relations given in Eq. (16) constrain the inhomogeneous part of the hadronic tensor to the generic form

$$T_{\text{H,inhom}}^{\mu\nu}(k, q) = -f_B \left[a g^{\mu\nu} + b \frac{k^\mu k^\nu}{k \cdot q} + c \frac{k^\mu q^\nu}{k \cdot q} + (1-b) \frac{q^\mu k^\nu}{q^2} + (1-a-c) \frac{q^\mu q^\nu}{q^2} \right], \quad (25)$$

where $a \equiv a(k^2, q^2)$, $b \equiv b(k^2, q^2)$, and $c \equiv c(k^2, q^2)$ are arbitrary real-valued coefficients. The Levi-Civita tensor is absent in this expression because it carries the wrong quantum numbers in light of the fact that the inhomogeneity is entirely due to the axial-vector part of Eq. (7). On account of Eq. (20), the inhomogeneous part of the pseudoscalar tensor furthermore takes the generic form

$$T_{P,\text{inhom}}^\mu(k, q) = -f_B m_B^2 \left[d \frac{k^\mu}{k \cdot q} + (1-d) \frac{q^\mu}{q^2} \right], \quad (26)$$

where $d \equiv d(k^2, q^2)$ is an arbitrary real-valued coefficient. Adopting the condition imposed in Eq. (22), we find that

$$d = \frac{(1+a+c)(k \cdot q) + b k^2}{m_B^2}, \quad (27)$$

which fixes $T_{P,\text{inhom}}^\mu(k, q)$ once $T_{\text{H,inhom}}^{\mu\nu}(k, q)$ is specified. We collect four different choices for the coefficients, labeled \mathcal{A} through \mathcal{D} , in Table I. With regard to the dispersive treatment of the form factors in this article, i.e., the requirement of their singularity-free structure, the question emerges what an appropriate choice for these coefficients is.

Among the inhomogeneous parts of the hadronic tensor listed in Table I, \mathcal{A} is the only choice that introduces a term singular in $[2(k \cdot q) + q^2] = (m_B^2 - k^2)$. It is evident that this k^2 -pole is associated with an intermediate B meson [20], as sketched in the left diagram of Fig. 1; see also Fig. 2. The choices \mathcal{B} and \mathcal{C} , on the other hand, introduce terms singular in $[(k \cdot q) + q^2]$ and $(k \cdot q)$, respectively, which correspond to q^2 -dependent pole positions in the variable k^2 ; these are not associated with any hadronic intermediate state and are therefore not of dynamic but of kinematic origin. Choice \mathcal{D} corresponds to a structure that is orthogonal to all BTT structures. This might lead to the presumption that it leaves the form factors of Eq. (24) unaffected and thus free of kinematic singularities. However, this choice exhibits a pole in q^2 , which erroneously suggests the emergence of a dynamic photon pole; working at fixed order in quantum electrodynamics, such a

²Note that for on-shell photons, only the form factors $\mathcal{F}_1(k^2, q^2)$ and $\mathcal{F}_4(k^2, q^2)$ contribute, which correspond to transverse polarizations.

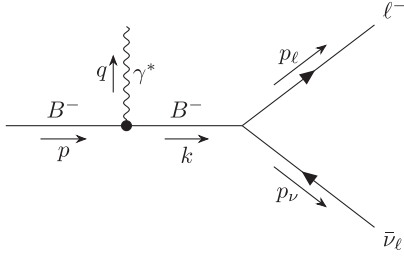


FIG. 2. Diagram illustrating the B -meson pole in the variable k^2 as part of the hadronic tensor $T_H^{\mu\nu}(k, q)$; see also the left diagram of Fig. 1.

$$|\overline{\mathcal{M}}(B^- \rightarrow \ell^- \bar{\nu}_\ell \gamma^*(\lambda))|^2 = \frac{e^2 G_F^2 |V_{ub}|^2}{2} \epsilon_\mu^*(q; \lambda) \epsilon_\alpha(q; \lambda) [T_H^{\mu\nu}(k, q) + T_{\text{FSR}}^{\mu\nu}(p_\ell, p_\nu, q)] [T_H^{\alpha\beta}(k, q) + T_{\text{FSR}}^{\alpha\beta}(p_\ell, p_\nu, q)]^\dagger \times \sum_{\text{spins}} L_\nu L_\beta^\dagger; \quad (28)$$

see Appendix D for details on the kinematics. For a longitudinal photon, $\lambda = 0$, this matrix element ought to vanish in the limit $q^2 \rightarrow 0$, i.e., for an on-shell photon. Using choice \mathcal{D} , one does, however, find that the matrix element diverges $\propto f_B^2$, independent of any choice of form factors. The discussion of such divergent contributions is not purely academic: in Ref. [5], a supposed collinear enhancement of the $B^- \rightarrow \ell^- \bar{\nu}_\ell \ell'^- \ell'^+$ decay rate is discussed, which is caused by such an unphysical behavior as $q^2 \rightarrow 0$. Therein, a different choice is made for the decomposition of the homogeneous tensor, in combination with choice \mathcal{D} for the inhomogeneous part and an inconsistent treatment of the charged lepton's finite mass in the FSR term. Using the formulas of Ref. [5] and our result for the FSR tensor, Eq. (13), we validate that treating the effects of a finite lepton mass consistently resolves this issue and removes the supposed contribution due to a longitudinal on-shell photon.³ This leads us to infer that the supposed collinear enhancement is not a physical feature of the $B^- \rightarrow \ell^- \bar{\nu}_\ell \ell'^- \ell'^+$ decay rate.

Moreover, we can draw conclusions from the results for the hadronic tensor in the decay $K^\pm \rightarrow \ell^\pm \nu_\ell \gamma^*(\rightarrow \ell'^- \ell'^+)$. An explicit calculation in chiral perturbation theory at next-to-leading order [16,17] confirms that choice \mathcal{A} yields form factors that are free of kinematic singularities. Transforming between choice \mathcal{A} and any other choice of Table I modifies the homogeneous part through introducing kinematic singularities. Consequently, the assumption that choice \mathcal{A} leads to form factors free of kinematic singularities unavoidably implies the emergence of such singularities for all the other choices considered here.

³After submitting our article for review, this has been confirmed to us by the authors of Ref. [5] and is revised in an Erratum.

pole cannot arise. In fact, the behavior $\propto 1/q^2$ would lead to a double pole $\propto 1/q^4$ in Eq. (23), a feature that is to be avoided in any amplitude. As a consequence of this double pole, choice \mathcal{D} is—in addition to the kinematic nature of the q^2 pole—disqualified by its effect on the longitudinal $B^- \rightarrow \ell^- \bar{\nu}_\ell \gamma^*$ helicity amplitude.

To further illustrate the effect that choice \mathcal{D} causes, we investigate the $B^- \rightarrow \ell^- \bar{\nu}_\ell \gamma^*$ amplitude in more detail. From Eqs. (3) and (11), one finds the squared spin-averaged amplitude for photons with polarization λ to be given by

Under some rather general, reasonable assumptions, it is possible to deduce that the inhomogeneous part of the hadronic tensor ought to be of the form

$$T_{\text{H,inhom}}^{\mu\nu}(k, q) = -f_B \left[\hat{a} g^{\mu\nu} + \frac{(2k^\mu + q^\mu)k^\nu + (1 - \hat{a})(2k^\mu + q^\mu)q^\nu}{2(k \cdot q) + q^2} \right] \quad (29)$$

in combination with the BTT basis of Eq. (24) for the homogeneous part. Here, \hat{a} is an arbitrary real-valued coefficient that does not depend on any of the momenta. The assumptions underlying the above form are the following:

- (i) there exists a unique choice for the coefficients in Eq. (25) that leaves the form factors free of kinematic singularities;
- (ii) the apparent kinematic poles in $T_{\text{H,inhom}}^{\mu\nu}(k, q)$ cancel and no new such poles are introduced;
- (iii) a dynamic B -meson pole appears at most in the pseudoscalar form factor $\mathcal{F}_3(k^2, q^2)$.

Consequently, the inhomogeneous part of the pseudoscalar tensor, Eq. (26), turns out to be given by

$$T_{P,\text{inhom}}^\mu(k, q) = -f_B \left[m_B^2 \frac{2k^\mu + q^\mu}{2(k \cdot q) + q^2} - (1 - \hat{a}) \frac{q^2 k^\mu - (k \cdot q) q^\mu}{2(k \cdot q) + q^2} \right]. \quad (30)$$

Assuming that $\hat{a} = 1$ meets the above requirements, it can be shown that any other choice of \hat{a} would introduce a dynamic pseudoscalar B -meson pole in the axial-vector form factors $\mathcal{F}_1(k^2, q^2)$ and $\mathcal{F}_2(k^2, q^2)$. Since $\hat{a} = 1$

corresponds to the choice \mathcal{A} from Table I, this gives further indication that \mathcal{A} is the proper choice for our analysis.

For the reasons stated above, we make \mathcal{A} the default choice in the following and parametrize the hadronic tensor as

$$T_{\text{H}}^{\mu\nu}(k, q) = T_{\text{H, hom}}^{\mu\nu}(k, q) - f_B \left[g^{\mu\nu} + \frac{(2k^\mu + q^\mu)k^\nu}{2(k \cdot q) + q^2} \right]. \quad (31)$$

This yields a total of six independent Lorentz structures, which form a basis; see the discussion in the appendix of Ref. [4]. Having such a basis of structures allows us to find projectors $\mathcal{P}_i^{\mu\nu}(k, q)$ that fulfill

$$\mathcal{P}_{i\mu\nu}(k, q) T_{\text{H}}^{\mu\nu}(k, q) = \begin{cases} \mathcal{F}_i(k^2, q^2), & i = 1, \dots, 4, \\ f_B/m_B, & i = 5, 6. \end{cases} \quad (32)$$

Explicit formulas for these projectors are provided in Appendix C.

V. DISPERSION RELATIONS AND z EXPANSION

We aim to parametrize the form factors $\mathcal{F}_i(k^2, q^2)$, $i = 1, \dots, 4$, in accordance with analyticity and unitarity. To this end, we split the form factors with respect to the photon's isospin according to $\mathcal{F}_i(k^2, q^2) = \mathcal{F}_i^{I=0}(k^2, q^2) + \mathcal{F}_i^{I=1}(k^2, q^2)$. For each component, we then establish a set of dispersion relations and assume the underlying discontinuities to be dominated by the one-body intermediate states ω and ρ , respectively, which allows us to relate the $B \rightarrow \gamma^*$ form factors to the $B \rightarrow V$, $V = \omega, \rho$, analogs. In doing so, we neglect contributions due to $B \rightarrow \phi$ in the isoscalar components for two reasons: first, these contributions are expected to be small due to the Okubo-Zweig-Iizuka mechanism [21–23], and second, we lack nonperturbative input for the $B \rightarrow \phi$ form factors. We also do not model contributions from further excited states, such as $\omega(1420)$ and $\rho(1450)$. As a consequence, we provide our nominal phenomenological results only in the region $q^2 \lesssim 1 \text{ GeV}^2$.

Based on Eq. (7), the discontinuity of the form factors with respect to q^2 and for fixed k^2 is given by [24,25]

$$\begin{aligned} \text{Disc}_{q^2}[Q_B \mathcal{F}_i(k^2, q^2)] &= \text{Disc}_{q^2}[\mathcal{P}_{i\mu\nu}(k, q) Q_B T_{\text{H}}^{\mu\nu}(k, q)] \\ &= \mathcal{P}_{i\mu\nu}(k, q) \left[i \sum_n \int d\tau_n (2\pi)^4 \delta^{(4)}(q - P_n) \langle 0 | J_{\text{EM}}^\mu(0) | n \rangle \langle n | J_{\text{H}}^\nu(0) | B^- \rangle \right]. \end{aligned} \quad (33)$$

Here, we use the n -body phase-space volume

$$d\tau_n = \prod_j \frac{d^3 p_j}{(2\pi)^3 2p_j^0} = \prod_j \frac{d^4 p_j}{(2\pi)^4} (2\pi) \delta(p_j^2 - M_j^2) \theta(p_j^0), \quad (34)$$

and $P_n = \sum_j p_j$ is the total momentum of the intermediate state. Assuming the discontinuities of the isoscalar and isovector components to be dominated by the one-body intermediate states ω and ρ , respectively, we use

$$\int d\tau_n (2\pi)^4 \delta^{(4)}(q - P_n) f(P_n) = 2\pi \delta(q^2 - M_n^2) f(q) \quad (35)$$

for the one-body phase-space volume to obtain

$$\text{Disc}_{q^2}[Q_B \mathcal{F}_i^I(k^2, q^2)] = \mathcal{P}_{i\mu\nu}(k, q) \left[2\pi i \sum_\lambda \delta(q^2 - M_V^2) \langle 0 | J_{\text{EM}}^\mu(0) | V(q, \lambda) \rangle \langle V(q, \lambda) | J_{\text{H}}^\nu(0) | B^- \rangle \right], \quad (36)$$

with $V = \omega$ for $I = 0$ and $V = \rho$ for $I = 1$. For the above matrix elements, we employ [9]

$$\begin{aligned} \langle 0 | J_{\text{EM}}^\mu(0) | V(q, \lambda) \rangle &= \frac{\eta^\mu}{c_V} d_V M_V f_V, \\ \langle V(q, \lambda) | J_{\text{H}}^\nu(0) | B^- \rangle &= \frac{\eta_\alpha^*}{c_V} [P_1^{\nu\alpha}(k, q) V^{B \rightarrow V}(k^2) + P_2^{\nu\alpha}(k, q) A_1^{B \rightarrow V}(k^2) + P_3^{\nu\alpha}(k, q) A_3^{B \rightarrow V}(k^2) + P_P^{\nu\alpha}(k, q) A_0^{B \rightarrow V}(k^2)], \end{aligned} \quad (37)$$

where the form factors $V^{B \rightarrow V}(k^2)$, $A_1^{B \rightarrow V}(k^2)$, $A_3^{B \rightarrow V}(k^2)$, and $A_0^{B \rightarrow V}(k^2)$ are given in the so-called traditional basis and account for a vector-, two axial-vector-, and a pseudoscalar-like $B \rightarrow V$ transition. Furthermore, $d_\omega = Q_u + Q_d = 1/3$, $d_\rho = Q_u - Q_d = 1$, and the composition of the ω and ρ wave function is accounted for by the factors $c_\omega = c_\rho = \sqrt{2}$.

TABLE II. The quantum numbers J^P , resonance masses m_{J^P} , and numerical values (rounded to two significant digits) of the series coefficients $\alpha_j^{F,V}$ [9] for the z expansion of the form factors $F^{B \rightarrow V}(k^2)$, truncated after three summands; see Eq. (42). The corresponding values of the resonance masses can be found in Appendix G. Because of parity conservation of the strong interactions, no form factor with $J^P = 0^+$ exists. For the exact numerical values of $\alpha_j^{F,V}$ and the covariances as well as correlations between these, see Ref. [9]. Note that $\alpha_0^{A_0^+,V}$ and $\alpha_0^{A_{12}^+,V}$ are not independent but have to fulfill the exact relation given in Eq. (40).

$F^{B \rightarrow V}(k^2)$	J^P	m_{J^P}	$\alpha_0^{F,\omega}$	$\alpha_1^{F,\omega}$	$\alpha_2^{F,\omega}$	$\alpha_0^{F,\rho}$	$\alpha_1^{F,\rho}$	$\alpha_2^{F,\rho}$
$V^{B \rightarrow V}(k^2)$	1^-	m_{B^*}	0.304(38)	-0.83(29)	1.7(1.2)	0.327(31)	-0.86(18)	1.80(97)
$A_1^{B \rightarrow V}(k^2)$	1^+	m_{B_1}	0.243(31)	0.34(24)	0.09(57)	0.262(26)	0.39(14)	0.16(41)
$A_{12}^{B \rightarrow V}(k^2)$	1^+	m_{B_1}	0.270(40)	0.66(26)	0.28(98)	0.297(35)	0.76(20)	0.46(76)
$A_0^{B \rightarrow V}(k^2)$	0^-	m_B	0.328(48)	-0.83(30)	1.4(1.2)	0.356(42)	-0.83(20)	1.3(1.0)

The decay constant of the respective vector meson is denoted by f_V , and $\eta^\mu \equiv \eta^\mu(q; \lambda)$ represents the polarization vector of the incoming vector meson with momentum q and polarization λ . The structures in Eq. (37) are given by [9]

$$\begin{aligned}
 P_1^{\nu\alpha} &= \frac{2i}{m_B + M_V} \epsilon^{\nu\alpha\beta\gamma} q_\beta k_\gamma, & P_2^{\nu\alpha} &= -\frac{1}{m_B - M_V} [(m_B^2 - M_V^2)g^{\nu\alpha} - (k^\nu + 2q^\nu)k^\alpha], \\
 P_3^{\nu\alpha} &= \frac{2M_V}{k^2} \left[k^\nu - \frac{k^2}{m_B^2 - M_V^2} (k^\nu + 2q^\nu) \right] k^\alpha, & P_P^{\nu\alpha} &= -\frac{2M_V}{k^2} k^\nu k^\alpha,
 \end{aligned} \tag{38}$$

where we adjusted the phases to our convention. Using the additional relation [9,26]

$$A_{12}^{B \rightarrow V}(k^2) = \frac{k^2(m_B + M_V)(m_B^2 - k^2 + 3M_V^2)A_1^{B \rightarrow V}(k^2) + 2M_V\lambda_V(k^2)A_3^{B \rightarrow V}(k^2)}{16m_B M_V^2(m_B + M_V)(m_B - M_V)}, \tag{39}$$

where $\lambda_V(k^2) \equiv \lambda(m_B^2, k^2, M_V^2)$, with $\lambda(x, y, z) = x^2 + y^2 + z^2 - 2(xy + xz + yz)$ the Källén function, we can express all form factors of Eq. (37) in terms of $V^{B \rightarrow V}(k^2)$, $A_1^{B \rightarrow V}(k^2)$, $A_{12}^{B \rightarrow V}(k^2)$, and $A_0^{B \rightarrow V}(k^2)$, which fulfill the exact relation [9]

$$A_0(0) = \frac{8m_B M_V A_{12}(0)}{m_B^2 - M_V^2}. \tag{40}$$

The generic parametrization of $F^{B \rightarrow V}(k^2) \in \{V(k^2), A_1(k^2), A_{12}(k^2), A_0(k^2)\}$ in terms of a series expansion in the conformal variable

$$z_V(t) = \frac{\sqrt{t_+ - t} - \sqrt{t_+ - t_0}}{\sqrt{t_+ - t} + \sqrt{t_+ - t_0}} \Big|_{V=\omega,\rho}, \tag{41}$$

with $t_0 = (1 - \sqrt{1 - t_-/t_+})t_+$ and $t_\pm = (m_B \pm M_V)^2$, is given by [9]

$$F^{B \rightarrow V}(k^2) = R_{J^P}(k^2) \sum_{j \geq 0} \alpha_j^{F,V} [z_V(k^2) - z_V(0)]^j, \tag{42}$$

where the series is truncated after three summands; this truncation is imposed on us by the $B \rightarrow V$ parameters provided in Ref. [9]. Here, the expansion takes into account the dominant subthreshold poles of the $B \rightarrow V$ form factors through the term $R_{J^P} = (1 - k^2/m_{J^P}^2)^{-1}$, where J^P refers to the angular-momentum and parity quantum number of the respective form factor (see Table II).

The isoscalar and isovector form factors can then be reconstructed from

$$Q_B \mathcal{F}_i^I(k^2, q^2) = \frac{1}{2\pi i} \int_{s_{\text{thr}}}^{\infty} ds \frac{\text{Disc}_s [Q_B \mathcal{F}_i^I(k^2, s)]}{s - q^2}, \tag{43}$$

where $s_{\text{thr}} = 9M_\pi^2, 4M_\pi^2$ for $I = 0, 1$, respectively. In the above, no subtractions are needed for convergence, since the discontinuities drop off as $1/q^2$ asymptotically; see Appendix E. Inserting Eq. (36) into Eq. (43) and using the polarization sum of the ω and ρ mesons,

$$\sum_\lambda \eta_\mu(q; \lambda) \eta_\nu^*(q; \lambda) = -g_{\mu\nu} + \frac{q_\mu q_\nu}{M_V^2}, \tag{44}$$

we obtain the VMD result for the $B \rightarrow \gamma^*$ form factors,

$$\begin{aligned}
Q_B \mathcal{F}_1^I(k^2, q^2) &= m_B M_V f_V d_V \frac{16 m_B M_V^2 A_{12}^{B \rightarrow V}(k^2) - (m_B + M_V)(m_B^2 - k^2 - M_V^2) A_1^{B \rightarrow V}(k^2)}{\lambda_V(k^2)(q^2 - M_V^2)}, \\
Q_B \mathcal{F}_2^I(k^2, q^2) &= 2 m_B M_V f_V d_V \frac{4 m_B (m_B^2 - k^2 - M_V^2) A_{12}^{B \rightarrow V}(k^2) - (m_B + M_V) k^2 A_1^{B \rightarrow V}(k^2)}{\lambda_V(k^2)(q^2 - M_V^2)}, \\
Q_B \mathcal{F}_3^I(k^2, q^2) &= m_B f_V d_V \frac{A_0^{B \rightarrow V}}{q^2 - M_V^2}, \\
Q_B \mathcal{F}_4^I(k^2, q^2) &= m_B M_V f_V d_V \frac{V^{B \rightarrow V}(k^2)}{(m_B + M_V)(q^2 - M_V^2)}. \tag{45}
\end{aligned}$$

Compared to $\mathcal{F}_1(k^2, q^2)$ and $\mathcal{F}_4(k^2, q^2)$, the form factors $\mathcal{F}_2(k^2, q^2)$ and $\mathcal{F}_3(k^2, q^2)$ enter observables with a relative suppression factor of q^2 , thereby ensuring that unphysical longitudinal on-shell photons do not contribute.

Naturally, we now aim to use an expansion similar to Eq. (42) for the $B \rightarrow \gamma^*$ form factors,

$$Q_B \mathcal{F}_i^I(k^2, q^2) = R_{J^P}(k^2) \sum_{j \geq 0} \beta_{i,j}^V(q^2) [z_V(k^2) - z_V(0)]^j, \tag{46}$$

where the form factors have definite angular-momentum and parity assignments, with the term $R_{J^P}(k^2)$ again accounting for the dominant subthreshold poles in the variable k^2 . In contrast to Eq. (42), the series coefficients have a dependence on q^2 , for which we will assume VMD and use an *ad hoc* Breit-Wigner (BW) ansatz with the resonance's width inserted by hand,

$$\beta_{i,j}^V(q^2) = N_{i,j}^V P_V^{\text{BW}}(q^2). \tag{47}$$

At this, it is justified to use a monopolelike ansatz because the form factors drop off as $1/q^2$ asymptotically; see Appendix E. Because of its smallness, we use a constant approximation for the ω decay width above the 3π threshold, whereas we incorporate the broad ρ width energy-dependently,

$$\begin{aligned}
P_\omega^{\text{BW}}(q^2) &= \frac{M_\omega^2}{M_\omega^2 - q^2 - i M_\omega \Gamma_\omega}, \\
P_\rho^{\text{BW}}(q^2) &= \frac{M_\rho^2}{M_\rho^2 - q^2 - i \sqrt{q^2} \Gamma_\rho(q^2)}. \tag{48}
\end{aligned}$$

Here, the proper threshold behavior is implied for the ω , i.e., $\Gamma_\omega = 0$ for $q^2 < 9M_\pi^2$, and the energy-dependent width of the ρ is parametrized according to [27]

$$\begin{aligned}
\Gamma_\rho(q^2) &= \theta(q^2 - 4M_\pi^2) \frac{\gamma_{\rho \rightarrow \pi\pi}(q^2)}{\gamma_{\rho \rightarrow \pi\pi}(M_\rho^2)} \Gamma_\rho, \\
\gamma_{\rho \rightarrow \pi\pi}(q^2) &= \frac{(q^2 - 4M_\pi^2)^{3/2}}{q^2}. \tag{49}
\end{aligned}$$

The normalizations $N_{i,j}^V$ can be determined from Eq. (45) by inserting Eqs. (42) and (46) and using the numerical values from Table II to match at $q^2 = 0$, resulting in Table III. The full form factors are then given by

$$\begin{aligned}
Q_B \mathcal{F}_i(k^2, q^2) &= Q_B [\mathcal{F}_i^{I=0}(k^2, q^2) + \mathcal{F}_i^{I=1}(k^2, q^2)] \\
&= R_{J^P}(k^2) \sum_{\substack{V=\omega,\rho \\ j \geq 0}} N_{i,j}^V P_V^{\text{BW}}(q^2) [z_V(k^2) - z_V(0)]^j. \tag{50}
\end{aligned}$$

TABLE III. The quantum numbers J^P , resonance masses m_{J^P} , and numerical values (rounded to two significant digits) of the normalizations $N_{i,j}^V$ for the z expansion of the form factors $\mathcal{F}_i(k^2, q^2)$, truncated after three summands; see Eq. (46). The corresponding values of the resonance masses can be found in Appendix G. For the covariances between the normalizations, see Appendix F. Note that $N_{2,0}^V$ and $N_{3,0}^V$ are identical due to the exact relation given in Eq. (40) or, equivalently, the condition $\mathcal{F}_2(0, q^2) = \mathcal{F}_3(0, q^2)$ imposed below Eq. (24).

$\mathcal{F}_i(k^2, q^2)$	J^P	m_{J^P}	$N_{i,0}^\omega$	$N_{i,1}^\omega$	$N_{i,2}^\omega$	$N_{i,0}^\rho$	$N_{i,1}^\rho$	$N_{i,2}^\rho$
$\mathcal{F}_1(k^2, q^2)$	1^+	m_{B_1}	0.0156(30)	-0.033(19)	0.003(85)	0.0557(88)	-0.115(48)	0.01(24)
$\mathcal{F}_2(k^2, q^2)$	1^+	m_{B_1}	-0.186(27)	0.39(14)	-0.17(52)	-0.676(79)	1.34(41)	-0.6(1.5)
$\mathcal{F}_3(k^2, q^2)$	0^-	m_B	-0.186(27)	0.47(17)	-0.80(71)	-0.676(79)	1.58(39)	-2.5(2.0)
$\mathcal{F}_4(k^2, q^2)$	1^-	m_{B^*}	-0.0222(28)	0.061(21)	-0.125(91)	-0.0795(75)	0.209(44)	-0.44(23)

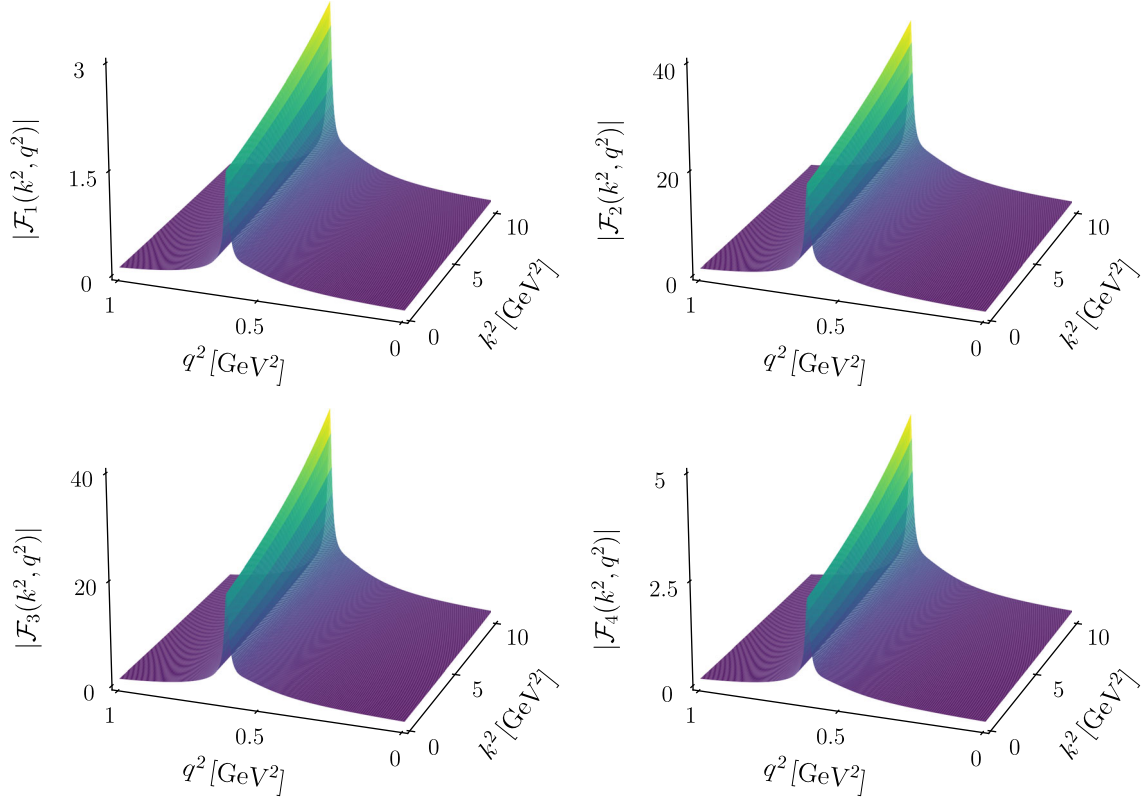


FIG. 3. Three-dimensional plots showing the absolute values of the full form factors, Eq. (50), in the range $k^2 \in [0, 10]$ GeV² and $q^2 \in [0, 1]$ GeV². The peak of the ω resonance is clearly visible, while the ρ resonance is lower in magnitude and hardly discernible here.

We present three-dimensional plots of the absolute values of the full form factors, Eq. (50), in Fig. 3. In addition, we present two-dimensional plots in Fig. 4, where we also show the absolute values of the isoscalar and isovector components separately, Eq. (46), including uncertainties and with $k^2 = 1$ GeV fixed.

VI. PHENOMENOLOGY

The decay $B^- \rightarrow \ell^- \bar{\nu}_\ell \ell'^- \ell'^+$ provides a rich phenomenology through a large number of angular observables.

They arise from the differential decay width $d\Gamma \equiv d\Gamma(B^- \rightarrow \ell^- \bar{\nu}_\ell \ell'^- \ell'^+)$, which is given by

$$d\Gamma = \frac{1}{2m_B} |\overline{\mathcal{M}}|^2 d\Phi_4(p; p_\ell, p_\nu, q_1, q_2), \quad (51)$$

where $|\overline{\mathcal{M}}|^2 \equiv |\overline{\mathcal{M}}(B^- \rightarrow \ell^- \bar{\nu}_\ell \ell'^- \ell'^+)|^2$ is the squared spin average of Eq. (23). The Lorentz-invariant four-body phase space is conveniently split according to [28]

$$d\Phi_4(p; p_\ell, p_\nu, q_1, q_2) = d\Phi_2(p; k, q) d\Phi_2(k; p_\ell, p_\nu) d\Phi_2(q; q_1, q_2) \frac{dk^2 dq^2}{2\pi 2\pi}. \quad (52)$$

Here, $d\Phi_2(p; k, q)$, $d\Phi_2(k; p_\ell, p_\nu)$, and $d\Phi_2(q; q_1, q_2)$ are the respective Lorentz-invariant two-body phase space measures of the subsystems $\{\ell^- \bar{\nu}_\ell(k), \gamma^*(q)\}$, $\{\ell^-(p_\ell), \bar{\nu}_\ell(p_\nu)\}$, and $\{\ell'^-(q_1), \ell'^+(q_2)\}$. The fivefold differential decay rate reads

$$\frac{d^5\Gamma}{dk^2 dq^2 d\cos\vartheta_W d\cos\vartheta_\gamma d\varphi} = \frac{|\mathbf{p}_\gamma| |\mathbf{p}_\ell| |\mathbf{p}_{\ell'}|}{4096 m_B^2 \pi^6 \sqrt{k^2} \sqrt{q^2}} |\overline{\mathcal{M}}|^2, \quad (53)$$

where ϑ_W is the polar angle of $\ell^-(p_\ell)$ in the center-of-mass system (CMS) $\{\ell^-(p_\ell), \bar{\nu}_\ell(p_\nu)\}$, ϑ_γ is the polar angle of $\ell'^-(q_1)$ in the CMS $\{\ell'^-(q_1), \ell'^+(q_2)\}$, and φ is the relative azimuthal angle between the planes of these two subsystems. Moreover, $|\mathbf{p}_\gamma|$, $|\mathbf{p}_\ell|$, and $|\mathbf{p}_{\ell'}|$ are the magnitudes of the three-momenta of the photon and the negatively charged leptons in the respective CMS; further details on the kinematics and the four-body phase space are provided in Appendix D. The angular integrations can be performed analytically, leading to

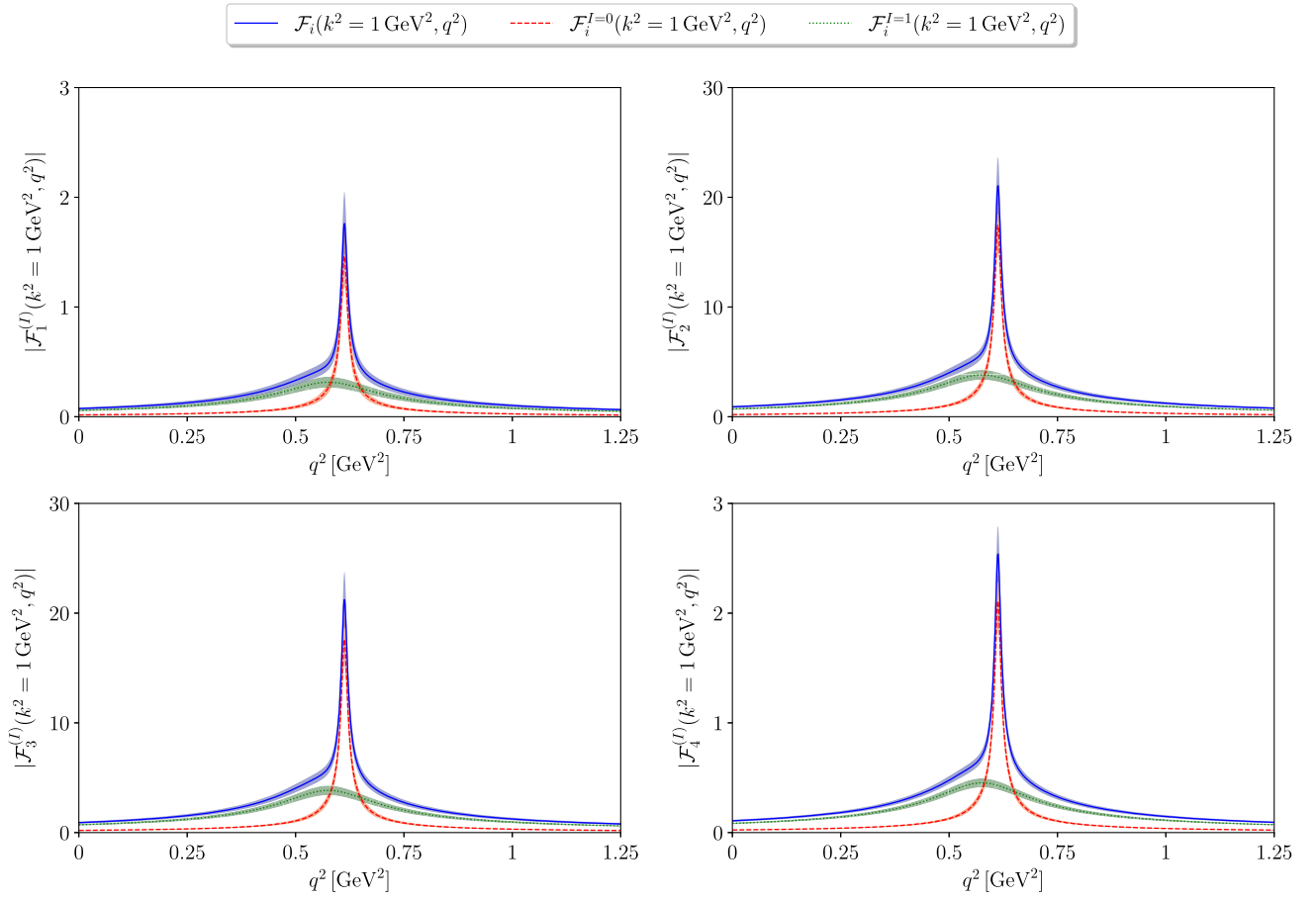


FIG. 4. Two-dimensional plots of the absolute values of the form factors' isoscalar and isovector components as well as the sum of these for $k^2 = 1 \text{ GeV}$ fixed in the range $q^2 \in [0, 1.25] \text{ GeV}$. We additionally show the uncertainties of the corresponding contributions.

$$\frac{d^2\Gamma}{dk^2 dq^2} = \mathcal{N} \left[\sum_{i=1}^4 \frac{f_{i,i}}{m_B^2} |\mathcal{F}_i(k^2, q^2)|^2 + 2 \sum_{\substack{i=1 \\ j>i}}^4 \frac{f_{i,j}}{m_B^2} \text{Re}[\mathcal{F}_i(k^2, q^2) \mathcal{F}_j^*(k^2, q^2)] + 2f_B \sum_{i=1}^4 \frac{f_{i,5}}{m_B} \text{Re}[\mathcal{F}_i(k^2, q^2)] + f_{5,5} f_B^2 \right],$$

$$\mathcal{N} = \frac{G_F^2 |V_{ub}|^2 e^4 |\mathbf{p}_\gamma| |\mathbf{p}_\ell| |\mathbf{p}_{\ell'}|}{8192 m_B^2 \pi^6 \sqrt{k^2} \sqrt{q^{10}}}, \quad (54)$$

where an additional dependence of the lepton masses $m_{\ell^{(\prime)}}$ in the functions $f_{i,j} \equiv f_{i,j}(k^2, q^2)$ is omitted. We collect the resulting expressions for these functions in Appendix F. The remaining integrations over k^2 and q^2 have to be performed numerically,

$$\Gamma = \int dq^2 \int dk^2 \frac{d^2\Gamma}{dk^2 dq^2}, \quad (55)$$

where the available phase space is bounded by $k^2 \in [m_\ell^2, (m_B - \sqrt{q^2})^2]$ and $q^2 \in [4m_\ell^2, (m_B - m_\ell)^2]$. Our results will be quoted for the branching ratio, $\mathcal{B} = \Gamma \tau_B / \hbar$, where τ_B is the lifetime of the charged B meson.

Beyond the integrated decay rate, another observable of interest is the FB asymmetry. It provides a complementary probe of the form factors as compared to the decay width and is defined as

$$A_{\text{FB}}(k^2, q^2) = \left(\frac{d^2\Gamma}{dk^2 dq^2} \right)^{-1} \int d \cos \vartheta_W \text{sgn}[\cos \vartheta_W] \times \frac{d^3\Gamma}{dk^2 dq^2 d \cos \vartheta_W}. \quad (56)$$

As for the decay width, the integration over the angle(s) can be performed analytically, with the result

$$\begin{aligned}
A_{\text{FB}}(k^2, q^2) = & \left(\frac{d^2\Gamma}{dk^2 dq^2} \right)^{-1} \mathcal{N} \left[\sum_{i=1}^4 \frac{g_{i,i}}{m_B^2} |\mathcal{F}_i(k^2, q^2)|^2 + 2 \sum_{\substack{i=1 \\ j>i}}^4 \frac{g_{i,j}}{m_B^2} \text{Re}[\mathcal{F}_i(k^2, q^2) \mathcal{F}_j^*(k^2, q^2)] \right. \\
& \left. + 2f_B \sum_{i=1}^4 \frac{g_{i,5}}{m_B} \text{Re}[\mathcal{F}_i(k^2, q^2)] + g_{5,5} f_B^2 \right], \quad (57)
\end{aligned}$$

where the functions $g_{i,j} \equiv g_{i,j}(k^2, q^2)$ also depend on the lepton masses $m_{\ell^{(i)}}$. The resulting expressions for these functions are collected in Appendix F. Experimentally, it is convenient to access the integrated asymmetry, which is defined as

$$\langle A_{\text{FB}}(k^2, q^2) \rangle = \left\langle \frac{d^2\Gamma}{dk^2 dq^2} \right\rangle^{-1} \int d \cos \vartheta_W \text{sgn}[\cos \vartheta_W] \left\langle \frac{d^3\Gamma}{dk^2 dq^2 d \cos \vartheta_W} \right\rangle, \quad (58)$$

where $\langle \dots \rangle$ denotes the integration over a suitable bin in the kinematic variables k^2 and q^2 .

We provide numerical results for both observables for the processes $B^- \rightarrow \ell^- \bar{\nu}_\ell \ell'^- \ell'^+$ with $\ell \in \{e, \mu, \tau\}$ and $\ell' \in \{e, \mu\}$ in Table IV. Decays involving a $\tau^- \tau^+$ pair are not considered here, since the ditau threshold is large compared to our self-imposed upper cutoff in the variable q^2 . We do not provide results for the decay with $\ell' = \ell$ either; see the discussion at the end of Sec. III. Our results are obtained

- (i) after integrating over the full phase space in k^2 and q^2 ;
- (ii) after integrating over the phase space with an upper cutoff at $q^2 = 1 \text{ GeV}^2$.

Beyond the q^2 cutoff, the absence of the modeling of the ϕ and further resonances introduces a hardly quantifiable model uncertainty. The latter variant therefore provides our nominal results. Modeling the contributions beyond the cutoff seems possible in light of similar efforts in the case of $B \rightarrow \pi\pi$ form factors [29,30] and is left for future work.

VII. SUMMARY AND OUTLOOK

In this article, we use dispersive methods to study the $B^- \rightarrow \ell^- \bar{\nu}_\ell \ell'^- \ell'^+$, γ^* form factors underlying the decay $B^- \rightarrow \ell^- \bar{\nu}_\ell \ell'^- \ell'^+$,

TABLE IV. Numerical results for the branching ratio and FB asymmetry [see Eqs. (55) and (58)] for $B^- \rightarrow \ell^- \bar{\nu}_\ell \ell'^- \ell'^+$ in the SM. The quoted uncertainties originate from the parametric uncertainties on the normalizations $N_{i,j}^V$ and V_{ub} , respectively. Because of the absence of CP violation in the SM, the results for the CP -conjugated decay modes are identical. Within uncertainties, our predictions for the branching ratio of the process $B^- \rightarrow e^- \bar{\nu}_e \mu^- \mu^+$ agree well with Ref. [5], $\mathcal{B}(B^- \rightarrow e^- \bar{\nu}_e \mu^- \mu^+) = \{3.01 \times 10^{-8}, 2.96 \times 10^{-8}\}$, without and with an upper cutoff, respectively. For the process $B^- \rightarrow \mu^- \bar{\nu}_\mu e^- e^+$, however, our results are in strong tension with Ref. [5], $\mathcal{B}(B^- \rightarrow \mu^- \bar{\nu}_\mu e^- e^+) = \{6.38 \times 10^{-7}, 6.37 \times 10^{-7}\}$, which can be attributed to the unphysical collinear enhancement inferred therein^a (see the discussion in Sec. IV). The results of Ref. [4], Table 2, are—within their uncertainties—compatible with our results; note the numerically insignificant impact of the slight difference in the upper integration boundary used therein.

Process	Upper cutoff q^2	\mathcal{B}	A_{FB}
$B^- \rightarrow e^- \bar{\nu}_e \mu^- \mu^+$	None	$3.19(43)_N (25)_{V_{ub}} \times 10^{-8}$	$-0.358(31)_N$
	1 GeV ²	$3.13(42)_N (25)_{V_{ub}} \times 10^{-8}$	$-0.361(32)_N$
$B^- \rightarrow \mu^- \bar{\nu}_\mu e^- e^+$	None	$3.78(47)_N (30)_{V_{ub}} \times 10^{-8}$	$-0.398(38)_N$
	1 GeV ²	$3.72(46)_N (30)_{V_{ub}} \times 10^{-8}$	$-0.401(38)_N$
$B^- \rightarrow \tau^- \bar{\nu}_\tau e^- e^+$	None	$2.75(27)_N (22)_{V_{ub}} \times 10^{-8}$	$-0.500(18)_N$
	1 GeV ²	$2.72(27)_N (22)_{V_{ub}} \times 10^{-8}$	$-0.502(18)_N$
$B^- \rightarrow \tau^- \bar{\nu}_\tau \mu^- \mu^+$	None	$1.77(23)_N (14)_{V_{ub}} \times 10^{-8}$	$-0.458(15)_N$
	1 GeV ²	$1.75(23)_N (14)_{V_{ub}} \times 10^{-8}$	$-0.460(15)_N$

^aThe tension with our result for the electron channel is reduced but not removed entirely with the results quoted in the Erratum to Ref. [5].

where we limit our analysis to the case $\ell' \neq \ell$. We separate the full $B^- \rightarrow \ell^- \bar{\nu}_\ell \ell'^- \ell'^+$ amplitude into a nonperturbative hadronic tensor and a perturbative FSR piece and, in doing so, thoroughly investigate the properties of these individual objects. One of the major advances of our analysis is to treat nonzero lepton masses consistently in the FSR piece at all stages. The separation of the full amplitude into a hadronic tensor and an FSR piece leads to an ambiguity with regard to the dispersive treatment. More specifically, it hinders one to find a decomposition into Lorentz structures and form factors that are free of kinematic singularities. As a remedy, we discuss in great detail how the hadronic tensor can be split into a homogeneous and an inhomogeneous part, with the homogeneous part being chosen such that it contains form factors with well-separated angular-momentum and parity quantum numbers. From this, we propose a decomposition of the homogeneous part of the hadronic tensor into a set of Lorentz structures and four form factors that are free of kinematic singularities in both the weak momentum and the photon momentum. This renders possible a dispersive treatment of the form factors. For the parametrization of the inhomogeneous part, we consider several choices from the literature and investigate their effect on the full amplitude in great detail, in particular with regard to the singularity-free property of the form factors. Moreover, we find that the inhomogeneous part needs to be of a specific form under a few reasonable assumptions. These considerations allow us to eliminate all except for one choice for the inhomogeneous part from the literature, which we consequently fix for the remainder of our analysis.

Having found a decomposition of the hadronic tensor into four form factors that are free of kinematic singularities, we split the form factors into their isospin components and establish a set of dispersion relations that relate the $B \rightarrow \gamma^*$ form factors to the well-known $B \rightarrow V$, $V = \omega, \rho$, analogs. The $B \rightarrow V$ form factors are expanded in a series in the conformal variable $z(t)$, with the dominant sub-threshold poles taken into account via a pole factor. Performing a similar series expansion for the $B \rightarrow \gamma^*$ form factors and using a VMD ansatz for the virtual photon, we are able to parametrize these form factors reliably below the onset of the ϕ .

Using our framework, we perform a phenomenological analysis by means of two observables: the branching ratio and the FB asymmetry. The numerical results for these quantities are given for $\ell \neq \ell'$ and agree with previous determinations from the literature.

Possible future improvements of our framework involve the inclusion of the ϕ contribution and replacing the resonant ρ by a description of the two-pion intermediate state, in which the ρ can be included model-independently through pion-pion rescattering [31]. The $B \rightarrow \gamma^*$ form factors are then obtained via a dispersion relation in a similar way to the reconstruction of, e.g., the $\eta^{(\prime)}$ transition form factors from $\pi\pi$ intermediate states [32,33].

ACKNOWLEDGMENTS

We are grateful to Yaroslav Kuli for helping with the translation of Ref. [20] from Russian to English. We further thank Martin Beneke, Philipp B er, Philip L ughausen, M eril Reboud, and K. Keri Vos for useful discussions. Financial support by the DFG through the funds provided to the Sino-German Collaborative Research Center TRR110 ‘‘Symmetries and the Emergence of Structure in QCD’’ (DFG Project-ID No. 196253076—TRR 110) is gratefully acknowledged. The work of S. K. and D. v. D. was further supported by the DFG within the Emmy Noether Programme under Grant No. DY-130/1-1.

APPENDIX A: INHOMOGENEOUS TENSOR IDENTITIES

In this appendix, we derive the identities for the hadronic tensor $T_H^{\mu\nu}(k, q)$ and pseudoscalar tensor $T_P^\mu(k, q)$ given in Eqs. (17) and (19).

1. Hadronic tensor

We start by using translational invariance of the vacuum to rewrite the hadronic tensor, Eq. (7), as

$$Q_B T_H^{\mu\nu}(k, q) = \int d^4x e^{ikx} \langle 0 | T \{ J_H^\nu(x) J_{EM}^\mu(0) \} | B^- \rangle. \quad (\text{A1})$$

By means of an integration by parts, a differentiation of the Heaviside step function in the time-ordered product and the Dirac equation, we find

$$\begin{aligned} k_\nu [Q_B T_H^{\mu\nu}(k, q)] \\ = Q_B T_P^\mu(k, q) + i \int d^3x e^{-ikx} \langle 0 | [J_H^0(\bar{x}), J_{EM}^\mu(0)] | B^- \rangle, \end{aligned} \quad (\text{A2})$$

where $\bar{x} = (x^0 = 0, \mathbf{x})$. In the above, we furthermore used that a scalar-vector current-current matrix element of type B meson to vacuum vanishes due to the involved quantum numbers, $\langle 0 | T \{ J_S(x) J_{EM}^\mu(0) \} | B^- \rangle = 0$, $J_S(x) = \bar{u}(x)b(x)$. From an explicit calculation of the commutator in Eq. (A2), we finally arrive at

$$k_\nu T_H^{\mu\nu}(k, q) = T_P^\mu(k, q) + f_B(k+q)^\mu, \quad (\text{A3})$$

which is equivalent to Eq. (17) after inserting the decomposition of the hadronic tensor into its homogeneous and inhomogeneous parts, $T_H^{\mu\nu}(k, q) = T_{H,\text{hom}}^{\mu\nu}(k, q) + T_{H,\text{inhom}}^{\mu\nu}(k, q)$; see Eq. (16).

2. Pseudoscalar tensor

For the pseudoscalar tensor, we proceed similarly and use the definition in Eq. (18) to calculate

$$q_\mu [Q_B T_P^\mu(k, q)] = i \int d^3x e^{-iqx} \langle 0 | [J_{\text{EM}}^0(\bar{x}), J_P(0)] | B^- \rangle. \quad (\text{A4})$$

An explicit calculation of the commutator results in Eq. (19),

$$q_\mu T_P^\mu(k, q) = -f_B m_B^2. \quad (\text{A5})$$

APPENDIX B: BARDEEN-TUNG-TARRACH PROCEDURE

In this appendix, we outline the modification to the BTT procedure [10,11] that leads us to the decomposition of the homogeneous part of the hadronic tensor into Lorentz structures and form factors given in Eq. (24). To this end, we recall that the homogeneous part fulfills

$$q_\mu T_{\text{H,hom}}^{\mu\nu}(k, q) = 0, \quad (\text{B1})$$

and that we additionally impose

$$k_\nu T_{\text{H,hom}}^{\mu\nu}(k, q) \stackrel{!}{=} T_{P,\text{hom}}^\mu(k, q) \quad (\text{B2})$$

[see Eqs. (16) and (21)] with $q_\mu T_{P,\text{hom}}^\mu(k, q) = 0$. Hence, we can split $T_{\text{H,hom}}^{\mu\nu}(k, q)$ according to

$$T_{\text{H,hom}}^{\mu\nu}(k, q) = \tilde{T}_{\text{H,hom}}^{\mu\nu}(k, q) + T_{P,\text{hom}}^\mu(k, q) \frac{k^\nu}{k^2}, \quad (\text{B3})$$

where $q_\mu \tilde{T}_{\text{H,hom}}^{\mu\nu}(k, q) = k_\nu \tilde{T}_{\text{H,hom}}^{\mu\nu}(k, q) = 0$. In the above, $T_{P,\text{hom}}^\mu(k, q)$ necessarily comes with a factor k^ν/k^2 due to its pseudoscalar nature; cf. the fact that the spin-0 component of a spin-1 field is of timelike polarization. Since the explicit k^2 -pole attached to $T_{P,\text{hom}}^\mu(k, q)$ is thus an inherent feature of the pseudoscalar contribution, it needs to be regularized either by a zero in the accompanying form factor or by a corresponding contribution within $\tilde{T}_{\text{H,hom}}^{\mu\nu}(k, q)$. We follow the latter approach: we perform the BTT procedure for $T_{P,\text{hom}}^\mu(k, q)$ and $\tilde{T}_{\text{H,hom}}^{\mu\nu}(k, q)$ separately, where we use the native blueprint for the former and a variant that introduces an explicit k^2 -pole to cancel the aforementioned pole of the pseudoscalar contribution for the latter.

We first perform the BTT procedure for $T_{P,\text{hom}}^\mu(k, q)$, where the only available building blocks for the Lorentz structures are

$$\{L_{P,\text{hom},i}^\mu\} = \{k^\mu, q^\mu\} \quad (\text{B4})$$

and gauge invariance in the form $q_\mu T_{P,\text{hom}}^\mu(k, q) = 0$ is imposed by means of

$$\{\tilde{L}_{P,\text{hom},i}^\mu\} = \mathcal{I}^\mu_\alpha \{L_{P,\text{hom},i}^\alpha\}, \quad \mathcal{I}^{\mu\nu} = g^{\mu\nu} - \frac{k^\mu q^\nu}{k \cdot q}. \quad (\text{B5})$$

The resulting set

$$\{\tilde{L}_{P,\text{hom},i}^\mu\} = \left\{ 0, q^\mu - \frac{q^2}{k \cdot q} k^\mu \right\} \quad (\text{B6})$$

consists of a single nonvanishing structure with a pole in $(k \cdot q)$. Following the regular procedure, this irreducible pole is to be eliminated by multiplying with $(k \cdot q)$, leading to the structure

$$\hat{L}_{P,\text{hom}}^\mu = (k \cdot q) q^\mu - q^2 k^\mu. \quad (\text{B7})$$

To perform the BTT procedure for $\tilde{T}_{\text{H,hom}}^{\mu\nu}(k, q)$, we note that the interaction is of the form $V - A$. Hence, the available building blocks for the Lorentz structures are given by

$$\{L_{\text{H,hom},i}^{\mu\nu}\} = \{g^{\mu\nu}, k^\mu k^\nu, k^\mu q^\nu, q^\mu k^\nu, q^\mu q^\nu, \epsilon^{\mu\nu\alpha\beta} k_\rho q_\sigma\}, \quad (\text{B8})$$

and we impose $q_\mu \tilde{T}_{\text{H,hom}}^{\mu\nu}(k, q) = k_\nu \tilde{T}_{\text{H,hom}}^{\mu\nu}(k, q) = 0$ by means of

$$\{\tilde{L}_{\text{H,hom},i}^{\mu\nu}\} = \mathcal{I}^{\mu\nu}_\alpha \{L_{\text{H,hom},i}^{\alpha\beta}\} \tilde{\mathcal{I}}_{\beta\nu}, \quad \tilde{\mathcal{I}}^{\mu\nu} = g^{\mu\nu} - \frac{k^\mu k^\nu}{k^2}. \quad (\text{B9})$$

The resulting set

$$\{\tilde{L}_{\text{H,hom},i}^{\mu\nu}\} = \left\{ g^{\mu\nu} - \frac{k^\mu q^\nu}{k \cdot q}, 0, 0, 0, \frac{q^2}{k^2} k^\mu k^\nu - \frac{q^2}{k \cdot q} k^\mu q^\nu - \frac{k \cdot q}{k^2} q^\mu k^\nu + q^\mu q^\nu, \epsilon^{\mu\nu\rho\sigma} k_\rho q_\sigma \right\} \quad (\text{B10})$$

contains structures with poles in $(k \cdot q)$ as well as k^2 . While we explicitly keep the k^2 poles, as mentioned above, we get rid of one of the two poles in $(k \cdot q)$ by following the regular procedure, i.e., by taking an appropriate linear combination with nonsingular coefficients and multiplying the remaining pole by $(k \cdot q)$. This leads to the minimal [10,11] set

$$\begin{aligned} \{\hat{L}_{\text{H,hom},i}^{\mu\nu}\} &= \left\{ (k \cdot q) \tilde{L}_{\text{H,hom},1}^{\mu\nu}, \tilde{L}_{\text{H,hom},5}^{\mu\nu} - q^2 \tilde{L}_{\text{H,hom},1}^{\mu\nu}, \tilde{L}_{\text{H,hom},6}^{\mu\nu} \right\} \\ &= \left\{ (k \cdot q) g^{\mu\nu} - k^\mu q^\nu, \frac{q^2}{k^2} k^\mu k^\nu - \frac{k \cdot q}{k^2} q^\mu k^\nu + q^\mu q^\nu - q^2 g^{\mu\nu}, \epsilon^{\mu\nu\rho\sigma} k_\rho q_\sigma \right\}. \end{aligned} \quad (\text{B11})$$

Combining Eqs. (B7) and (B11) with Eq. (B3), the homogeneous part of the hadronic tensor thus takes the form given in Eq. (24).⁴

APPENDIX C: FORM FACTOR PROJECTORS

In this appendix, we collect the formulas for the projectors $\mathcal{P}_i^{\mu\nu}(k, q)$ that fulfill $\mathcal{P}_{i\mu\nu}(k, q)T_H^{\mu\nu}(k, q) = \mathcal{F}_i(k^2, q^2)$, $i = 1, \dots, 4$, and $\mathcal{P}_{i\mu\nu}(k, q)T_H^{\mu\nu}(k, q) = f_B/m_B$, $i = 5, 6$, for an arbitrary choice of basis for $T_H^{\mu\nu}(k, q)$, as introduced in Sec. III [34–37]:

$$\begin{aligned}
\frac{1}{m_B}\mathcal{P}_1^{\mu\nu}(k, q) &= \frac{k \cdot q}{2[(k \cdot q)^2 - k^2 q^2]} g^{\mu\nu} + \frac{3q^2(k \cdot q)}{2[(k \cdot q)^2 - k^2 q^2]^2} k^\mu k^\nu - \frac{(k \cdot q)^2 + 2k^2 q^2}{2[(k \cdot q)^2 - k^2 q^2]^2} k^\mu q^\nu \\
&\quad - \frac{3(k \cdot q)^2}{2[(k \cdot q)^2 - k^2 q^2]^2} q^\mu k^\nu + \frac{3k^2(k \cdot q)}{2[(k \cdot q)^2 - k^2 q^2]^2} q^\mu q^\nu, \\
\frac{1}{m_B}\mathcal{P}_2^{\mu\nu}(k, q) &= \frac{k^2}{2[(k \cdot q)^2 - k^2 q^2]} g^{\mu\nu} + \frac{2(k \cdot q)^2 + k^2 q^2}{2[(k \cdot q)^2 - k^2 q^2]^2} k^\mu k^\nu - \frac{3k^2(k \cdot q)}{2[(k \cdot q)^2 - k^2 q^2]^2} k^\mu q^\nu \\
&\quad - \frac{3k^2(k \cdot q)}{2[(k \cdot q)^2 - k^2 q^2]^2} q^\mu k^\nu + \frac{3k^4}{2[(k \cdot q)^2 - k^2 q^2]^2} q^\mu q^\nu, \\
\frac{1}{m_B}\mathcal{P}_3^{\mu\nu}(k, q) &= \frac{1}{(k \cdot q)^2 - k^2 q^2} k^\mu k^\nu - \frac{2k^2}{[(k \cdot q)^2 - k^2 q^2][2(k \cdot q) + q^2]} q^\mu k^\nu - \frac{k^2}{[(k \cdot q)^2 - k^2 q^2][2(k \cdot q) + q^2]} q^\mu q^\nu, \\
\frac{1}{m_B}\mathcal{P}_4^{\mu\nu}(k, q) &= -\frac{i}{2[(k \cdot q)^2 - k^2 q^2]} \epsilon^{\mu\nu\rho\sigma} k_\rho q_\sigma, \\
m_B\mathcal{P}_5^{\mu\nu}(k, q) &= -\frac{k \cdot q}{(k \cdot q)^2 - k^2 q^2} q^\mu k^\nu + \frac{k^2}{(k \cdot q)^2 - k^2 q^2} q^\mu q^\nu, \\
m_B\mathcal{P}_6^{\mu\nu}(k, q) &= \frac{q^2}{(k \cdot q)^2 - k^2 q^2} q^\mu k^\nu - \frac{k \cdot q}{(k \cdot q)^2 - k^2 q^2} q^\mu q^\nu. \tag{C1}
\end{aligned}$$

At this, an ambiguity is hidden in how to collect the terms of the inhomogeneous part into basis structures in Eq. (31), since such different choices will lead to another set of projectors than the ones given above. However, any difference $\bar{\mathcal{P}}_i^{\mu\nu}(k, q)$ between two sets of valid projectors is at most of the form

$$\bar{\mathcal{P}}_i^{\mu\nu}(k, q) = A_i q^\mu [k^\nu [(k \cdot q) + q^2] - q^\nu [(k \cdot q) + k^2]] \tag{C2}$$

for $i = 3, 5, 6$, with some coefficient $A_i \equiv A_i(k^2, q^2)$, so that

$$\begin{aligned}
\bar{\mathcal{P}}_{i\mu\nu}(k, q)T_{H,\text{hom}}^{\mu\nu}(k, q) &= A_i [q_\mu T_{H,\text{hom}}^{\mu\nu}(k, q)] [k_\nu [(k \cdot q) + q^2] - q_\nu [(k \cdot q) + k^2]] = 0, \\
\bar{\mathcal{P}}_{i\mu\nu}(k, q)T_{H,\text{inhom}}^{\mu\nu}(k, q) &= A_i [q_\mu T_{H,\text{inhom}}^{\mu\nu}(k, q)] [k_\nu [(k \cdot q) + q^2] - q_\nu [(k \cdot q) + k^2]] \\
&= A_i [-f_B(k + q)^\nu] [k_\nu [(k \cdot q) + q^2] - q_\nu [(k \cdot q) + k^2]] = 0. \tag{C3}
\end{aligned}$$

For $i = 1, 2, 4$, the projectors are independent of this choice, i.e., $A_i = 0$.

APPENDIX D: KINEMATICS

In this appendix, we present some details on the kinematics for the processes $B^- \rightarrow \ell^- \bar{\nu}_\ell \gamma^*$ and $B^- \rightarrow \ell^- \bar{\nu}_\ell \ell'^- \ell'^+$, which are necessary ingredients to calculate the squared spin-averaged amplitudes $|\overline{\mathcal{M}}(B^- \rightarrow \ell^- \bar{\nu}_\ell \gamma^*)|^2$ in Eq. (28) and $|\overline{\mathcal{M}}(B^- \rightarrow \ell^- \bar{\nu}_\ell \ell'^- \ell'^+)|^2$ in Sec. VI.

⁴Note that for the decay of an electrically neutral B meson, as opposed to the case of a charged B meson considered in this article, no inhomogeneous contribution, Eq. (16), is present. As a consequence, in this scenario, the associated form factors are readily free of kinematic singularities in k^2 and q^2 as well as kinematic zeros in q^2 but contain an explicit kinematic zero in k^2 due to the singularities in the structures.

1. $B^- \rightarrow \ell^- \bar{\nu}_\ell \gamma^*$

For a consistent treatment of the kinematics in the process $B^- \rightarrow \ell^- \bar{\nu}_\ell \gamma^*$, all momenta and polarization vectors have to be evaluated in a single frame of reference. To this end, we calculate the corresponding quantities in the CMS of the $\{\ell^- \bar{\nu}_\ell(k), \gamma^*(q)\}$ and $\{\ell^-(p_\ell), \bar{\nu}_\ell(p_\nu)\}$ subsystem and perform a Lorentz transformation of the latter to the former frame.

In the CMS $\{\ell^- \bar{\nu}_\ell(k), \gamma^*(q)\}$, one finds the magnitude of the photon's three-momentum and the energies

$$|\mathbf{p}_\gamma| = \frac{\sqrt{\lambda(m_B^2, k^2, q^2)}}{2m_B}, \quad E_{\ell\nu} = \frac{m_B^2 + k^2 - q^2}{2m_B},$$

$$E_\gamma = \frac{m_B^2 - k^2 + q^2}{2m_B}. \quad (\text{D1})$$

The four-momentum of the leptonic subsystem thus reads

$$k = (E_{\ell\nu}, 0, 0, |\mathbf{p}_\gamma|)^T, \quad (\text{D2})$$

and, accordingly, the four-momentum of the photon and its polarization vectors are given by

$$q = (E_\gamma, 0, 0, -|\mathbf{p}_\gamma|)^T,$$

$$\epsilon(q; \lambda = \pm 1) = \mp \frac{1}{\sqrt{2}} (0, 1, \mp i, 0)^T,$$

$$\epsilon(q; \lambda = 0) = \frac{1}{\xi} (-|\mathbf{p}_\gamma|, 0, 0, E_\gamma)^T,$$

$$\epsilon(q; \lambda = T) = \frac{1}{\xi} (E_\gamma, 0, 0, -|\mathbf{p}_\gamma|)^T, \quad (\text{D3})$$

where any physical observable necessarily needs to be independent of $\xi = \sqrt{q^2}$.

In the CMS $\{\ell^-(p_\ell), \bar{\nu}_\ell(p_\nu)\}$, we have

$$|\mathbf{p}_\ell| = \frac{k^2 - m_\ell^2}{2\sqrt{k^2}}, \quad E_\ell = \frac{k^2 + m_\ell^2}{2\sqrt{k^2}}, \quad E_\nu = \frac{k^2 - m_\ell^2}{2\sqrt{k^2}} \quad (\text{D4})$$

for the magnitude of the negatively charged lepton's three-momentum and the corresponding energies. Hence, transforming the subsystem $\{\ell^-(p_\ell), \bar{\nu}_\ell(p_\nu)\}$ to the CMS $\{\ell^- \bar{\nu}_\ell(k), \gamma^*(q)\}$, the four-momenta of the leptons are found to be

$$p_\ell = \begin{pmatrix} \gamma_{\ell\nu,\gamma} (E_\ell + \beta_{\ell\nu,\gamma} |\mathbf{p}_\ell| \cos \vartheta_W) \\ |\mathbf{p}_\ell| \sin \vartheta_W \\ 0 \\ \gamma_{\ell\nu,\gamma} (\beta_{\ell\nu,\gamma} E_\ell + |\mathbf{p}_\ell| \cos \vartheta_W) \end{pmatrix},$$

$$p_\nu = \begin{pmatrix} \gamma_{\ell\nu,\gamma} (E_\nu - \beta_{\ell\nu,\gamma} |\mathbf{p}_\ell| \cos \vartheta_W) \\ -|\mathbf{p}_\ell| \sin \vartheta_W \\ 0 \\ \gamma_{\ell\nu,\gamma} (\beta_{\ell\nu,\gamma} E_\nu - |\mathbf{p}_\ell| \cos \vartheta_W) \end{pmatrix}, \quad (\text{D5})$$

where $\beta_{\ell\nu,\gamma} = |\mathbf{p}_\gamma|/E_{\ell\nu}$, $\gamma_{\ell\nu,\gamma} = (1 - \beta_{\ell\nu,\gamma}^2)^{-1/2}$, and ϑ_W is the polar angle of $\ell^-(p_\ell)$ in the CMS $\{\ell^-(p_\ell), \bar{\nu}_\ell(p_\nu)\}$.

2. $B^- \rightarrow \ell^- \bar{\nu}_\ell \ell'^- \ell'^+$

In addition to the magnitudes of three-momenta $|\mathbf{p}_\gamma|$ and $|\mathbf{p}_\ell|$ in the CMS $\{\ell^- \bar{\nu}_\ell(k), \gamma^*(q)\}$ and $\{\ell^-(p_\ell), \bar{\nu}_\ell(p_\nu)\}$, respectively, we need the three-momentum of $\ell'^-(q_1)$ in the CMS $\{\ell'^-(q_1), \ell'^+(q_2)\}$ to describe the kinematics of the process $B^- \rightarrow \ell^- \bar{\nu}_\ell \ell'^- \ell'^+$,

$$|\mathbf{p}_{\ell'}| = \frac{\sqrt{q^2 - 4m_{\ell'}^2}}{2}. \quad (\text{D6})$$

Furthermore, two additional angles besides ϑ_W are necessary here: the polar angle ϑ_γ of $\ell'^-(q_1)$ in the CMS $\{\ell'^-(q_1), \ell'^+(q_2)\}$ and the azimuthal angle φ between the decay planes of the subsystems $\{\ell^-(p_\ell), \bar{\nu}_\ell(p_\nu)\}$ and $\{\ell'^-(q_1), \ell'^+(q_2)\}$ (see Fig. 5).

For the four-body phase space, we used

$$d\Phi_4(p; p_\ell, p_\nu, q_1, q_2) = d\Phi_2(p; k, q) d\Phi_2(k; p_\ell, p_\nu) \\ \times d\Phi_2(q; q_1, q_2) \frac{dk^2 dq^2}{2\pi 2\pi} \quad (\text{D7})$$

in Eq. (52), where

$$d\Phi_2(p; k, q) = \frac{1}{16\pi^2} \frac{|\mathbf{p}_\gamma|}{m_B} d\Omega_B,$$

$$d\Phi_2(k; p_\ell, p_\nu) = \frac{1}{16\pi^2} \frac{|\mathbf{p}_\ell|}{\sqrt{k^2}} d\Omega_W,$$

$$d\Phi_2(q; q_1, q_2) = \frac{1}{16\pi^2} \frac{|\mathbf{p}_{\ell'}|}{\sqrt{q^2}} d\Omega_\gamma \quad (\text{D8})$$

are the two-body phase spaces of the subsystems $\{\ell^- \bar{\nu}_\ell(k), \gamma^*(q)\}$, $\{\ell^-(p_\ell), \bar{\nu}_\ell(p_\nu)\}$, and $\{\ell'^-(q_1), \ell'^+(q_2)\}$, respectively. Here, $d\Omega_B$, $d\Omega_W$, and $d\Omega_\gamma$ denote the differential solid angles in the corresponding CMS. Three of the six angular integrations can be rendered trivial to carry out by rotating the coordinate system appropriately, leading to the expression

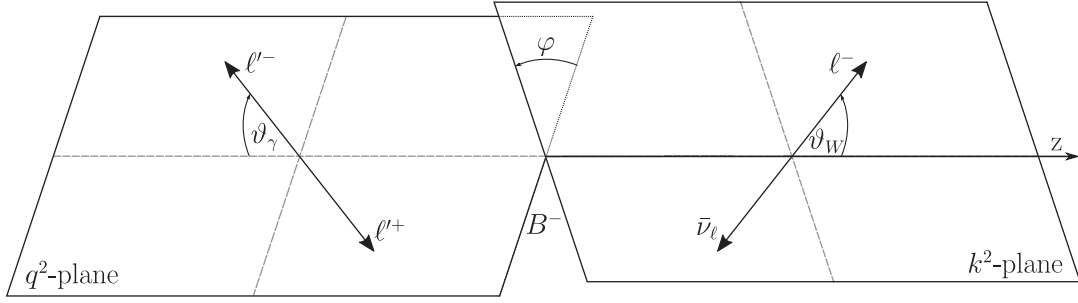


FIG. 5. Illustration of the decay $B^- \rightarrow \ell^- \bar{\nu}_\ell \ell'^- \ell'^+$ along with the two decay planes of the leptonic subsystems and the three angles necessary to describe the kinematics of the process.

$$d\Phi_4(p; p_\ell, p_\nu, q_1, q_2) = \frac{1}{2048\pi^6} \frac{|\mathbf{p}_\gamma| |\mathbf{p}_\ell| |\mathbf{p}_{\ell'}|}{m_B \sqrt{k^2} \sqrt{q^2}} d \cos \vartheta_W d \cos \vartheta_\gamma d\varphi dk^2 dq^2 \quad (\text{D9})$$

for the four-body phase space, with the remaining angles being as illustrated in Fig. 5.

APPENDIX E: ASYMPTOTICS

In this appendix, we show that the form factors $\mathcal{F}_i^I(k^2, q^2)$ introduced in Sec. V as well as their

discontinuities drop off as $1/q^2$ asymptotically. This behavior was assumed to avoid subtracting the dispersion relation of Eq. (43) and justified the monopolelike ansatz for the form factors in Eq. (47). We determine the form factors' asymptotic behavior for $q^2 \rightarrow \infty$ by inspecting the results of a calculation of the $B \rightarrow \gamma$ form factors within an operator product expansion (OPE) [15]. For our purposes, it suffices to inspect the leading-power terms within this OPE, which are diagrammatically depicted in Fig. 6. The OPE uses an interpolating quark current for the B meson, namely [15] $J_B(x) = \bar{u}(x)\gamma_5 b(x)$, which fulfills $\langle 0|J_B(0)|B^- \rangle = -im_B^2 f_B/(m_b + m_u)$. We then calculate the sum of the two diagrams depicted in Fig. 6, leading to

$$X_{\mu\nu}^I(k, q) = e \int \frac{d^4 l}{(2\pi)^4} \text{Tr} \left[-\gamma_5 \frac{i(\not{l} - \not{q} + m_u)}{(l-q)^2 - m_u^2} Q_u^I \gamma_\mu \frac{i(\not{l} + m_u)}{l^2 - m_u^2} \gamma_\nu (1 - \gamma_5) \frac{i(\not{l} + \not{k} + m_b)}{(l+k)^2 - m_b^2} - \gamma_5 \frac{i(\not{l} - \not{k} + m_u)}{(l-k)^2 - m_u^2} \gamma_\nu (1 - \gamma_5) \frac{i(\not{l} + m_b)}{l^2 - m_b^2} Q_b^I \gamma_\mu \frac{i(\not{l} + \not{q} + m_b)}{(l+q)^2 - m_b^2} \right], \quad (\text{E1})$$

where l is the loop momentum and $q^2 < 0$ large. The isospin charges are given by $(Q_u^{I=0}, Q_b^{I=0}) = (1/6, -1/3)$ and $(Q_u^{I=1}, Q_b^{I=1}) = (1/2, 0)$.

For the discontinuities, it then follows that

$$\text{Disc}_{q^2} \mathcal{F}_i^{I,\text{OPE}}(k^2, q^2) \propto \text{Disc}_{q^2} [\mathcal{P}_i^{\mu\nu}(k, q) X_{\mu\nu}^I(k, q)], \quad (\text{E2})$$

so that the asymptotic behavior for large $q^2 < 0$ is found to be given by [37]

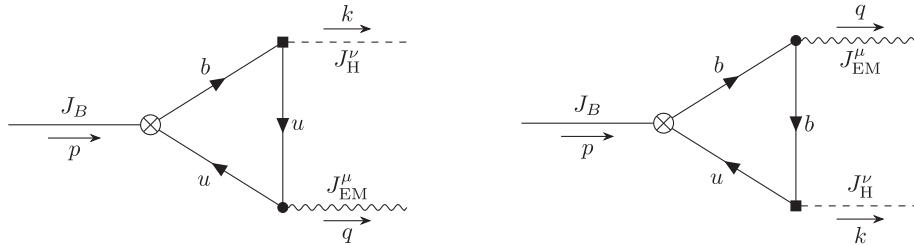


FIG. 6. The leading-order diagrams in the OPE for the form factors $\mathcal{F}_i^I(k^2, q^2)$. Diagrams contributing at a higher order in the OPE are neglected here.

$$\text{Disc}_{q^2} \mathcal{F}_i^{I,\text{OPE}}(k^2, q^2) \sim 1/q^2, \quad (\text{E3})$$

rendering the dispersion integrals convergent without any subtractions.

Similarly, we find

$$\mathcal{F}_i^{I,\text{OPE}}(k^2, q^2) \sim 1/q^2 \quad (\text{E4})$$

for the asymptotic behavior of the form factors, so that a monopolelike ansatz in the framework of VMD is justified.

APPENDIX F: INTERMEDIATE RESULTS

In this appendix, we collect the covariance matrices for the normalizations $N_{i,j}^V$ from Table III and the functions $f_{i,j}$ as well as $g_{i,j}$ introduced in Eqs. (54) and (57).

1. Covariance matrices

For reasons of consistency with the rounding of the uncertainties on the normalizations, we round the numerical values in the covariance matrices to four significant digits. Because of the fact that the input used to determine the normalizations does not exhibit a correlation between the parameters of the ω and ρ , the normalizations $N_{i,j}^\omega$ and $N_{i,j}^\rho$ are uncorrelated, i.e., $\text{Cov}(N_{i,j}^\omega, N_{k,l}^\rho) = 0$ for all i, j, k, l , so that our results can be collected in two (12×12) matrices.

For the covariances between the normalizations $N_{i,j}^\omega$, we find

$$10^6 \times \text{Cov}(N_{i,j}^\omega, N_{k,l}^\omega)_{mn} = \begin{pmatrix} 9.186 & -11.29 & 66.84 & 16.05 & -65.26 & 739.2 & 16.05 & 57.91 & -371.5 & -7.348 & -37.43 & 135.1 \\ -11.29 & 378.7 & -1444 & -151.5 & 491.6 & -3209 & -151.5 & -186.7 & 1270 & 2.220 & -241.8 & 353.4 \\ 66.84 & -1444 & 7180 & 991.8 & -5858 & 24670 & 991.8 & -911.2 & -1778 & -6.404 & 558.3 & -1611 \\ 16.05 & -151.5 & 991.8 & 740.4 & -1134 & 7731 & 740.4 & 2429 & -6410 & 13.70 & 3.901 & 134.0 \\ -65.26 & 491.6 & -5858 & -1134 & 20370 & -52440 & -1134 & 14440 & -31960 & -9.187 & 986.6 & -2592 \\ 739.2 & -3209 & 24670 & 7731 & -52440 & 266600 & 7731 & -9322 & 46070 & -305.2 & -3351 & 16080 \\ 16.05 & -151.5 & 991.8 & 740.4 & -1134 & 7731 & 740.4 & 2429 & -6410 & 13.70 & 3.901 & 134.0 \\ 57.91 & -186.7 & -911.2 & 2429 & 14440 & -9322 & 2429 & 28910 & -63340 & 15.82 & 682.5 & 204.0 \\ -371.5 & 1270 & -1778 & -6410 & -31960 & 46070 & -6410 & -63340 & 498000 & 144.6 & -1346 & 13990 \\ -7.348 & 2.220 & -6.404 & 13.70 & -9.187 & -305.2 & 13.70 & 15.82 & 144.6 & 7.794 & 34.85 & -134.1 \\ -37.43 & -241.8 & 558.3 & 3.901 & 986.6 & -3351 & 3.901 & 682.5 & -1346 & 34.85 & 450.4 & -1108 \\ 135.1 & 353.4 & -1611 & 134.0 & -2592 & 16080 & 134.0 & 204.0 & 13990 & -134.1 & -1108 & 8249 \end{pmatrix}, \quad (\text{F1})$$

where $m = (3i + j - 2)$ and $n = (3k + l - 2)$ denote the rows and columns of the matrix, respectively. At this, it is to be noted that $N_{2,0}^\omega = N_{3,0}^\omega$ (see the discussion in Sec. V) so that one row and one column of the matrix is, in fact, redundant, reducing the degrees of freedom to an (11×11) matrix.

In the same way and with the analogous caveat $N_{2,0}^\rho = N_{3,0}^\rho$, we find the covariances between the normalizations $N_{i,j}^\rho$ to be given by

$$10^5 \times \text{Cov}(N_{i,j}^\rho, N_{k,l}^\rho)_{mn} = \begin{pmatrix} 7.758 & -25.35 & 132.8 & 17.88 & -47.77 & 705.8 & 17.88 & 70.38 & -233.2 & -5.403 & -18.46 & 46.61 \\ -25.35 & 231.1 & -988.0 & -151.1 & 393.9 & -3906 & -151.1 & -389.7 & 7.717 & 12.95 & -55.78 & -26.32 \\ 132.8 & -988.0 & 5543 & 1059 & -5304 & 26800 & 1059 & 411.8 & -3620 & -55.19 & -90.41 & -25.79 \\ 17.88 & -151.1 & 1059 & 631.5 & -1626 & 7978 & 631.5 & 1294 & -2278 & 9.762 & -23.75 & -12.89 \\ -47.77 & 393.9 & -5304 & -1626 & 17200 & -43390 & -1626 & 7476 & -12080 & -44.36 & 814.8 & -1798 \\ 705.8 & -3906 & 26800 & 7978 & -43390 & 224000 & 7978 & 2795 & 15740 & -248.9 & -2166 & 8948 \\ 17.88 & -151.1 & 1059 & 631.5 & -1626 & 7978 & 631.5 & 1294 & -2278 & 9.762 & -23.75 & -12.89 \\ 70.38 & -389.7 & 411.8 & 1294 & 7476 & 2795 & 1294 & 14980 & -16040 & -29.65 & 443.1 & 795.0 \\ -233.2 & 7.717 & -3620 & -2278 & -12080 & 15740 & -2278 & -16040 & 396500 & 42.62 & 123.5 & 27430 \\ -5.403 & 12.95 & -55.19 & 9.762 & -44.36 & -248.9 & 9.762 & -29.65 & 42.62 & 5.693 & 16.05 & -56.63 \\ -18.46 & -55.78 & -90.41 & -23.75 & 814.8 & -2166 & -23.75 & 443.1 & 123.5 & 16.05 & 197.2 & -383.9 \\ 46.61 & -26.32 & -25.79 & -12.89 & -1798 & 8948 & -12.89 & 795.0 & 27430 & -56.63 & -383.9 & 5497 \end{pmatrix}. \quad (\text{F2})$$

2. Functions f_{ij} and g_{ij}

For the functions $f_{i,j}$ introduced in Eq. (54), we obtain

$$\begin{aligned}
 f_{1,1} &= \frac{64\pi k_-^2 q_+^2 (k_+^2 + k^2) [\lambda(m_B^2, k^2, q^2) + 6k^2 q^2]}{9k^2}, & f_{2,2} &= \frac{32\pi k_-^2 q_+^2 q^2 (k_+^2 + k^2) [\lambda(m_B^2, k^2, q^2) + 12k^2 q^2]}{9k^4}, \\
 f_{3,3} &= m_\ell^2 \frac{32\pi k_-^2 q_+^2 q^2 \lambda(m_B^2, k^2, q^2)}{3k^4}, & f_{4,4} &= \frac{64\pi k_-^2 q_+^2 (k_+^2 + k^2) \lambda(m_B^2, k^2, q^2)}{9k^2}, \\
 f_{1,2} &= -\frac{64\pi k_-^2 q_+^2 q^2 (k_+^2 + k^2) \Delta(k^2, q^2)}{3k^2}
 \end{aligned} \tag{F3}$$

and

$$\begin{aligned}
 f_{1,5} &= m_\ell^2 \frac{128\pi q_+^2}{3k_-^2} [k_-^2 [\Delta(k^2, q^2) - k_+^2] - k_B^2 k^2 [\Delta(k^2, q^2) - 2m_\ell^2] L_D(k^2, q^2)], \\
 f_{2,5} &= -m_\ell^2 \frac{128\pi q_+^2 q^2}{3k_-^2} [3k_-^2 - [3k_B^2 k^2 + (k_-^2)^2] L_D(k^2, q^2)], \\
 f_{3,5} &= -m_\ell^2 \frac{64\pi q_+^2 q^2}{3k_B^2 k_-^2 k^2} [k_-^2 [k_-^2 \Delta(k^2, q^2) + 2k^2 (k_B^2 + 2k_-^2)] - 2k_B^2 k^2 (k_B^2 k^2 + k_-^2 k_+^2) L_D(k^2, q^2)], \\
 f_{4,5} &= -m_\ell^2 \frac{128\pi q_+^2}{3k_-^2} [k_-^2 \Delta(k^2, q^2) - k^2 [k_B^2 \Delta(k^2, q^2) - 2k_-^2 q^2] L_D(k^2, q^2)], \\
 f_{5,5} &= -m_\ell^2 \frac{128\pi q_+^2}{3(k_B^2)^2 k_-^2 [k_-^2 q^2 (k_B^2 + k_-^2) + m_\ell^2 (k_B^2)^2]} \\
 &\quad \times [k_-^2 [k_-^2 (k_B^2 + k_-^2) [k_B^2 - \Delta(k^2, q^2)] [4(k_-^2)^2 + k_-^2 [3k_B^2 + \Delta(k^2, q^2)] + 4(k_B^2)^2] \\
 &\quad + m_\ell^2 [4(k_-^2)^3 [k_B^2 - \Delta(k^2, q^2)] + 8k_B^2 (k_-^2)^2 [2k_B^2 - \Delta(k^2, q^2)] + (k_B^2)^2 k_-^2 [13k_B^2 - 5\Delta(k^2, q^2)] \\
 &\quad + 2(k_B^2)^3 [2k_B^2 - \Delta(k^2, q^2)] + 8m_\ell^4 (k_B^2)^2 (k_B^2 + k_-^2)] \\
 &\quad + 2k_B^2 k^2 [k_B^2 [\Delta(k^2, q^2) - 2k_B^2] - 2k_-^2 (k_B^2 + k_-^2) - 4m_\ell^2 (k_B^2 + k_-^2)] [k_-^2 q^2 (k_B^2 + k_-^2) + m_\ell^2 (k_B^2)^2] L_D(k^2, q^2)], \tag{F4}
 \end{aligned}$$

where we defined

$$\begin{aligned}
 k_B^2 &= m_B^2 - k^2, & k_\pm^2 &= k^2 \pm m_\ell^2, & q_\pm^2 &= q^2 + 2m_\ell^2, \\
 \Delta(k^2, q^2) &= k_B^2 - q^2, & L_D &= \frac{L_+(k^2, q^2) - L_-(k^2, q^2)}{\sqrt{\lambda(m_B^2, k^2, q^2)}}, & L_\pm(k^2, q^2) &= \log \left[1 \pm \frac{k_-^2 \sqrt{\lambda(m_B^2, k^2, q^2)}}{k_B^2 k_\pm^2 + k_-^2 q^2} \right]. \tag{F5}
 \end{aligned}$$

All other, unlisted functions vanish, i.e., $f_{1,3} = f_{1,4} = f_{2,3} = f_{2,4} = f_{3,4} = 0$. Given the scaling with the lepton mass, one finds that this set further reduces to four functions in the chiral limit $m_\ell = 0$.

For the functions $g_{i,j}$ introduced in Eq. (57), we similarly obtain

$$\begin{aligned}
 g_{1,3} &= m_\ell^2 \frac{32\pi k_-^2 q_+^2 q^2 \sqrt{\lambda(m_B^2, k^2, q^2)}}{3k^2}, & g_{1,4} &= \frac{32\pi k_-^2 q_+^2 \Delta(k^2, q^2) \sqrt{\lambda(m_B^2, k^2, q^2)}}{3}, \\
 g_{2,3} &= -m_\ell^2 \frac{16\pi k_-^2 q_+^2 q^2 \Delta(k^2, q^2) \sqrt{\lambda(m_B^2, k^2, q^2)}}{3k^4}, & g_{2,4} &= -\frac{64\pi k_-^2 q_+^2 q^2 \sqrt{\lambda(m_B^2, k^2, q^2)}}{3}
 \end{aligned} \tag{F6}$$

and

$$\begin{aligned}
g_{1,5} &= m_\ell^2 \frac{32\pi q_+^2}{3k_B^2 k_-^2} \left[2(k_-^2)^2 \sqrt{\lambda(m_B^2, k^2, q^2)} - 4(k_B^2)^2 k^2 [\Delta(k^2, q^2) - 2m_\ell^2] \tilde{L}_D(k^2, q^2) \right], \\
g_{2,5} &= m_\ell^2 \frac{32\pi q_+^2 q^2}{3k_B^2 k_-^2 k^2} \left[(k_-^2)^2 \sqrt{\lambda(m_B^2, k^2, q^2)} + 4k_B^2 k^2 [3k_B^2 k^2 + (k_-^2)^2] \tilde{L}_D(k^2, q^2) \right], \\
g_{3,5} &= m_\ell^2 \frac{128\pi q_+^2 q^2}{3k_-^2} (k_B^2 k^2 + k_+^2 k_-^2) \tilde{L}_D(k^2, q^2), \\
g_{4,5} &= m_\ell^2 \frac{128\pi k^2 q_+^2}{3k_-^2} [2k_-^2 [\Delta(k^2, q^2) - k_B^2] + k_B^2 \Delta(k^2, q^2)] \tilde{L}_D(k^2, q^2), \\
g_{5,5} &= m_\ell^2 \frac{256\pi k^2 q_+^2}{3k_B^2 k_-^2 [k_-^2 q^2 (k_B^2 + k_-^2) + m_\ell^2 (k_B^2)^2] [k_+^2 \Delta(k^2, q^2) + 2k^2 q^2]} \\
&\quad \times \left[k_B^2 (k_-^2)^2 (k_B^2 + k_-^2) (q^2 + 2m_\ell^2) \sqrt{\lambda(m_B^2, k^2, q^2)} + [k_+^2 \Delta(k^2, q^2) + 2k^2 q^2] [m_\ell^2 (k_B^2)^2 + k_-^2 q^2 (k_B^2 + k_-^2)] \right. \\
&\quad \left. \times [4m_\ell^2 (k_B^2 + k_-^2) + 2[(k_B^2)^2 + (k_-^2)^2 + k_B^2 k_-^2] - k_B^2 \Delta(k^2, q^2)] \tilde{L}_D(k^2, q^2) \right], \tag{F7}
\end{aligned}$$

where we additionally defined

$$\tilde{L}_D = \frac{1}{\sqrt{\lambda(m_B^2, k^2, q^2)}} \log \left[\frac{4k_-^2 k^2 q^2 (k_B^2 + k_-^2) + 4m_\ell^2 (k_B^2)^2 k^2}{[k_+^2 \Delta(k^2, q^2) + 2k^2 q^2]^2} \right]. \tag{F8}$$

All other, unlisted functions vanish, i.e., $g_{1,1} = g_{2,2} = g_{3,3} = g_{4,4} = g_{1,2} = g_{3,4} = 0$. Again, from the scaling with the lepton mass, one finds that this set further reduces to two functions in the chiral limit $m_\ell = 0$.

APPENDIX G: CONSTANTS AND PARAMETERS

We collect the constants and parameters used throughout our analysis in Table V.

TABLE V. The masses, widths, and other physical parameters needed for the calculations in this article.

Quantity	Variable	Value	Reference
Mass π^\pm	M_π	139.57039(18) MeV	[28]
Mass B^\pm	m_B	5279.34(12) MeV	[28]
Mass B^*	m_{B^*}	5324.71(21) MeV	[28]
Mass B_1	m_{B_1}	$5725.9_{-2.7}^{+2.5}$ MeV	[28]
Mass $\rho^0(770)$	M_ρ	775.26(23) MeV	[28]
Mass $\omega(782)$	M_ω	782.66(13) MeV	[28]
Lifetime B^\pm	τ_B	1638(4) fs	[28]
Width $\rho^0(770)$	Γ_ρ	147.4(8) MeV	[28]
Width $\omega(782)$	Γ_ω	8.68(13) MeV	[28]
Decay constant $\rho^0(770)$	f_ρ	216(3) MeV	[9]
Decay constant $\omega(782)$	f_ω	197(8) MeV	[9]
Decay constant B^\pm	f_B	190.0(1.3) MeV	[38–42]
CKM matrix element $b \rightarrow u$	$ V_{ub} $	$3.77(15) \times 10^{-3}$	[43]

- [1] M. Beneke and J. Rohrwild, *Eur. Phys. J. C* **71**, 1818 (2011).
- [2] Y.-M. Wang, *J. High Energy Phys.* **09** (2016) 159.
- [3] M. Beneke, V.M. Braun, Y. Ji, and Y.-B. Wei, *J. High Energy Phys.* **07** (2018) 154.
- [4] M. Beneke, P. B  er, P. Rigatos, and K. K. Vos, *Eur. Phys. J. C* **81**, 638 (2021).
- [5] M. A. Ivanov and D. Melikhov, *Phys. Rev. D* **105**, 014028 (2022).
- [6] J. Albrecht, E. Stamou, R. Ziegler, and R. Zwicky, *J. High Energy Phys.* **09** (2021) 139.
- [7] C. Wang, Y.-M. Wang, and Y.-B. Wei, *J. High Energy Phys.* **02** (2022) 141.
- [8] G. Colangelo, M. Hoferichter, and P. Stoffer, *J. High Energy Phys.* **02** (2019) 006.
- [9] A. Bharucha, D. M. Straub, and R. Zwicky, *J. High Energy Phys.* **08** (2016) 098.
- [10] W. A. Bardeen and W. K. Tung, *Phys. Rev.* **173**, 1423 (1968); **4**, 3229(E) (1971).
- [11] R. Tarrach, *Nuovo Cimento A* **28**, 409 (1975).
- [12] J. Aebischer, M. Fael, C. Greub, and J. Virto, *J. High Energy Phys.* **09** (2017) 158.
- [13] E. E. Jenkins, A. V. Manohar, and P. Stoffer, *J. High Energy Phys.* **03** (2018) 016.
- [14] A. Khodjamirian and D. Wyler, *From Integrable Models to Gauge Theories* (World Scientific, Singapore, 2002).
- [15] T. Janowski, B. Pullin, and R. Zwicky, *J. High Energy Phys.* **12** (2021) 008.
- [16] J. Bijnens, G. Ecker, and J. Gasser, *Nucl. Phys.* **B396**, 81 (1993).
- [17] J. Bijnens, G. Colangelo, G. Ecker, and J. Gasser, [arXiv: hep-ph/9411311](https://arxiv.org/abs/hep-ph/9411311).
- [18] P. B. Pal, [arXiv:physics/0703214](https://arxiv.org/abs/physics/0703214).
- [19] M. A. Ivanov and D. Melikhov, *Phys. Rev. D* **105**, 094038 (2022).
- [20] D. Y. Bardin and E. A. Ivanov, *Sov. J. Part. Nucl.* **7**, 286 (1976).
- [21] S. Okubo, *Phys. Lett.* **5**, 165 (1963).
- [22] G. Zweig, An $SU(3)$ model for strong interaction symmetry and its breaking. Version 2, in *Developments in the Quark Theory of Hadrons. Vol. 1. 1964–1978*, edited by D. B. Lichtenberg and S. P. Rosen (Hadronic Press, Nonantum, MA, 1964), pp. 22–101.
- [23] J. Iizuka, *Prog. Theor. Phys. Suppl.* **37**, 21 (1966).
- [24] P. Colangelo and A. Khodjamirian, QCD sum rules, a modern perspective, in *At The Frontier of Particle Physics*, edited by M. Shifman and B. Ioffe (World Scientific, Singapore, 2001), pp. 1495–1576,
- [25] A. Khodjamirian, *Hadron Form Factors: From Basic Phenomenology to QCD Sum Rules* (CRC Press, Taylor & Francis Group, Boca Raton, FL, USA, 2020).
- [26] R. R. Horgan, Z. Liu, S. Meinel, and M. Wingate, *Phys. Rev. D* **89**, 094501 (2014).
- [27] M. Zanke, M. Hoferichter, and B. Kubis, *J. High Energy Phys.* **07** (2021) 106.
- [28] P. A. Zyla *et al.* (Particle Data Group), *Prog. Theor. Exp. Phys.* **2020**, 083C01 (2020).
- [29] J. T. Daub, C. Hanhart, and B. Kubis, *J. High Energy Phys.* **02** (2016) 009.
- [30] S. Ropertz, C. Hanhart, and B. Kubis, *Eur. Phys. J. C* **78**, 1000 (2018).
- [31] X.-W. Kang, B. Kubis, C. Hanhart, and U.-G. Meißner, *Phys. Rev. D* **89**, 053015 (2014).
- [32] C. Hanhart, A. Kup  c, U.-G. Meißner, F. Stollenwerk, and A. Wirzba, *Eur. Phys. J. C* **73**, 2668 (2013); **75**, 242(E) (2015).
- [33] S. Holz, C. Hanhart, M. Hoferichter, and B. Kubis, *Eur. Phys. J. C* **82**, 434 (2022).
- [34] R. Mertig, M. B  hm, and A. Denner, *Comput. Phys. Commun.* **64**, 345 (1991).
- [35] V. Shtabovenko, R. Mertig, and F. Orellana, *Comput. Phys. Commun.* **207**, 432 (2016).
- [36] V. Shtabovenko, R. Mertig, and F. Orellana, *Comput. Phys. Commun.* **256**, 107478 (2020).
- [37] H. H. Patel, *Comput. Phys. Commun.* **197**, 276 (2015).
- [38] Y. Aoki *et al.* (Flavour Lattice Averaging Group (FLAG) Collaboration), *Eur. Phys. J. C* **82**, 869 (2022).
- [39] A. Bazavov *et al.* (TUMQCD, Fermilab Lattice, MILC Collaborations), in *13th Conference on the Intersections of Particle and Nuclear Physics* (2018), [arXiv:1810.00250](https://arxiv.org/abs/1810.00250).
- [40] A. Bussone *et al.* (ETM Collaboration), *Phys. Rev. D* **93**, 114505 (2016).
- [41] R. J. Dowdall, C. T. H. Davies, R. R. Horgan, C. J. Monahan, and J. Shigemitsu (HPQCD Collaboration), *Phys. Rev. Lett.* **110**, 222003 (2013).
- [42] C. Hughes, C. T. H. Davies, and C. J. Monahan, *Phys. Rev. D* **97**, 054509 (2018).
- [43] D. Lej  ak, B. Meli  c, and D. van Dyk, *J. High Energy Phys.* **07** (2021) 036.